THERMAL DIFFUSION
IN MODERATELY DENSE GAS MIXTURES

C. A. VELDS

THERMAL DIFFUSION
IN MODERATELY DENSE GAS MIXTURES

PROEFSCHRIFT

TER VERKRIJGING VAN DE GRAAD VAN DOCTOR IN DE WISKUNDE EN NATUURWETENSCHAPPEN AAN DE RIJKSUNIVERSITEIT TE LEIDEN, OP GEZAG VAN DE RECTOR MAGNIFICUS DR K. A. H. HIDDING, HOOGLERAAR IN DE FACULTEIT DER GODGELEERDHEID, TEN OVERSTAAN VAN EEN COMMISSIE UIT DE SENAAT TE VERDEDIGEN OP WOENSDAG, 7 DECEMBER, 1966, TE 16.00 UUR

DOOR

CAREL ANDRÉ VELDS

GEBOREN TE 'S-GRAVENHAGE IN 1929

DRUKKERIJ ELINKWIJK - UTRECHT

PROMOTOR: PROF. DR J. KISTEMAKER

STELLINGEN

1. Fast en Verrijp meten de inwendige demping van licht gedeformeerde ijzerdraden. Voor een temperatuur $< 240^{\circ}K$ nemen ze een toename van de demping als functie van de tijd waar; voor een temperatuur $> 240^{\circ}K$ wordt een afname gevonden. Deze beide verschijnselen worden aan verschillende mechanismen toegeschreven. Er zijn goede redenen te veronderstellen dat hier, op zijn minst gedeeltelijk slechts één mechanisme werkzaam is.

   J.D. Fast en M.B. Verrijp, Philips Res. Repts. 16 (1961) 51.

   M.E. Hermant, Proefschrift Univ. Amsterdam (1966).

2. Bij de aanslag van het 3^3D niveau van helium door elektronen wordt als belangrijk secondair proces de botsing tussen reeds aangeslagen helium atomen en helium deeltjes in de grondtoestand vermeld. Behalve dit secondair proces moet ook beschouwd worden de directe aanslag van de n F toestand door elektronen. Deze toestand gaat na cascade in 3^3D over.

   C.C. Lin en R.G. Fowler, Annals of Physics, 15 (1961) 461.

   R.M. St. John, F.L. Miller en C.C. Lin, Phys. Rev. 134 (1964) A888.

3. Tegen de conclusie die Popov trekt uit zijn experiment waarin een elektronenbundel met zeer sterke elektrische velden wordt gemoduleerd kunnen bezwaren worden aangevoerd.

   A.T. Popov, Sov. Phys. - Techn. Phys. 8 (1964) 625.

4. Bij de bepaling van diffusiecoëfficiënten volgens de gas-chromatografische methode van Giddings en Seager wordt de piekbreedte van een als deltavormige verstoring ingebrachte tweede component op een bepaald tijdstip gemeten. Het heeft zin deze methode te modificeren door de stroombuis te sluiten en de hoogte van de pieken te meten.

   G. Taylor, Proc. Roy. Soc. (Londen) A219 (1953) 186;
   A223 (1954) 446.

   J.C. Giddings en S.L. Seager, I. & E.C. Fundamentals 1 (1962) 277.

5. In tegenstelling met wat men op grond van een elementaire beschouwing zou verwachten hebben Waldmann en Kupatt een toename berekend van de diffusiecoëfficiënt van een Lorentzgas bestaande uit spindeeltjes onder invloed van een magneetveld. Hiervoor is een eenvoudige verklaring te geven.

   C.J. Gorter, Naturwissenschaften 26 (1938) 140.

   L. Waldmann en H.-D. Kupatt, Z. Naturforsch. 18a (1963) 86.

   D.W. Condiff, Wei-Kao Lu en J.S. Dahler, J. Chem. Phys. 42 (1965) 3445.

6. Het is te betreuren dat de afleiding voor de voortplanting van het geluid in een gas, bestaande uit z. g. "loaded spheres", volgens Jeans niet meer voorkomt in de nieuwste drukken van zijn boek "Dynamical theory of gases."
   J. H. Jeans, The dynamical theory of gases, University Press, Cambridge (1904) 302; 2nd edition (1916) 375.
   J. H. Jeans, The dynamical theory of gases, Dover publications, Inc. (1954).

7. Bij de beproeving van op intuïtieve basis ontworpen windvanen wordt doorgaans afwezigheid van richtmoment rondom het evenwichtspunt aangezien voor goede demping. Dit verklaart de populariteit van de V-vaan.
   E. Kleinschmidt, Handbuch der meteorologischen Instrumente und ihrer Auswertung, Springer, Berlin (1935)
   W. E. K. Middleton, A. F. Spilhaus, Meteorological instruments, University Press, Toronto (1953).

8. Een statistische analyse van de voetbaluitslagen in de eredivisie van de K. N. V. B. in de seizoenen 1956-1957 tot en met 1965-1966 bevestigt de vaak verkondigde mening dat het accent steeds meer op het voorkomen, dan op het maken van doelpunten wordt gelegd.

9. Wanneer men een verband zoekt tussen een piek in de luchtverontreinigingsconcentratie en het effect dat deze op korte termijn heeft op de mortaliteit moet men van te voren een bepaalde tijdslimiet vaststellen.
   K. Biersteker, Verontreinigde lucht, van Gorcum & Co N. V., Assen (1966).
   A. E. Martin, Monthly bull. Min of Health (London) 20 (1961) 42.

10. Het is wenselijk dat in het leerprogramma voor de kweekschool meer aandacht wordt besteed aan de verschijnselen van partiële leerstoornissen bij leerlingen van het lager onderwijs.

C. A. Velds
november 1966

Aan mijn ouders

Aan Eke

The work described in this thesis is part of the research program of the "Stichting voor Fundamenteel Onderzoek der Materie" (Foundation for Fundamental Research on Matter) and was made possible by financial support from the "Nederlandse Organisatie voor Zuiver-Wetenschappelijk Onderzoek" (Netherlands Organization for the Advancement of Pure Research) and the O. E. C. D. High Temperature Reactor project (Dragon) under contracts CON/WIN/5161 and CON/WIN/52318.

INTRODUCTION

If in a mixture of a given number of components in a homogeneous phase, initially with uniform concentrations, a temperature gradient is set up, a partial separation of the components will occur. This effect, which is called thermal diffusion, will celebrate its golden jubilee next year [1] and has still the attention of both experimentalists and theorists as it can provide data on the intermolecular potential. A review of what has been done during these fifty years can be found in literature by Grew and Ibbs [2], Grove [3] and Mason et al. [4].

The multiplication of the elementary effect in what is known as a thermal diffusion column is of a later date (Clusius and Dickel [5]). It has been used only as an application of thermal diffusion to produce highly enriched stable isotopes. As the multiplication factor is dependent on the column's geometry, which cannot be calculated exactly, only relative measurements can be made in a thermal diffusion column.

The theory and experiments investigate the dependence of thermal diffusion on the following parameters:

Temperature, which includes quantum effects at low temperature.

Pressure, including the low-pressure Knudsen region where collisions with the wall are of importance as well as the high-pressure region, where ternary molecular collisions are of account.

Composition, for example trace concentrations, closely connected with Lorentzian and quasi-Lorentzian mixtures.

Polyatomic molecules, giving rise to inelastic molecular collisions.

Intermolecular potential. Measurements over a large temperature range are required to determine the potential parameters.

Multicomponent mixtures.

For more information and references the reader is referred to the article written by Mason et al. [4].

This thesis deals with the pressure dependence of thermal diffusion above one atmosphere. The question was raised as to whether it would be feasible to use a thermal diffusion column to concentrate CO_2 impurities in helium gas at high pressure [6]. In the high-temperature graphite-moderated Dragon reactor (Winfrith, U.K.) very pure helium at 20 atm is used as a cooling gas. To avoid graphite corrosion and carbon deposition the impurity level of oxygen compounds in the helium must be below 0.05 p.p.m. As the instruments controlling the helium purity are working near the limit of their sensitivity, it is desirable to preconcentrate the CO_2 concentration with a known factor of about a hundred in as short a time possible.

For the design of the thermal diffusion column the thermal diffusion factor of trace components CO_2 in helium at higher densities should be known. To use the column for concentrating other impurities the thermal diffusion factors for other trace concentrations in helium should also be known. For this reason the thermal diffusion factors for He - $^{14}CO_2$ and He - ^{85}Kr up to 150 atm have been measured. As

trace components did not show an appreciable pressure dependence of α the field of research has been extended to higher CO_2 concentrations. It was expected that the non-ideality of the CO_2 might influence the thermal diffusion especially near the critical density of this component.

To date experiments on thermal diffusion at pressures above 1 atm have been rather scanty; they have been carried out in single-stage units and in thermal diffusion columns.

The experiments in the thermal diffusion column of Drickamer et al. [7] and Hirota [8] all show an increase in the separation as a function of pressure. Drickamer could explain this by a modification of the classical column theory of Furry, Jones and Onsager, introducing turbulence effects. In later experiments [9] he found a change of sign of α from positive to negative, which is not implied in the column theory. He ascribed this phenomenon to the formation of clusters, which could be predicted qualitatively by considerations on interaction energy. Hirota states that Drickamer's corrections to the column theory together with the pressure dependence of α according to Becker (see below) explain his experiments.

Experiments at high pressure in a two-bulb apparatus have been done by Becker and Schulzeff [10][11], by Drickamer [12], by Makita [13] and by Van Ee et al. [14]. Becker [11] demonstrated that the pressure dependence of α could be ascribed to the difference in ideality of the two gases. At the same time Haase [15] developed a theory on the basis of non-equilibrium thermodynamics by which he was able to explain the increase of α with pressure in Becker's experiments. Drickamer, who did measurements in the critical region, found that Haase's theory failed near the critical density of the mixture. Recently, Van Ee [14] reported that his experiments at low temperature could not be described by Haase's theory.

So far the only other theory giving an explicit expression for α at higher pressures is Enskog's modification of the Boltzmann equation [16], which Thorne has applied to thermal diffusion (ref. [17], p. 292).

Two new approaches for deriving expressions for the transport coefficients in terms of intermolecular forces, the distribution function method and the time-correlation method do not yet give explicit expressions for α [50].

VOORWOORD

Teneinde te voldoen aan de wens van de Faculteit der Wiskunde en Natuurwetenschappen volgt hier een kort overzicht van mijn studie.

Nadat ik in 1946 het einddiploma HBS-B aan het 1e Vrijzinnig Christelijk Lyceum te 's-Gravenhage had behaald begon ik mijn studie aan de Technische Hogeschool te Delft. In 1951 liet ik mij als student inschrijven aan de Rijksuniversiteit te Leiden, waarna ik in 1956 het candidaatsexamen wis- en natuurkunde D en in 1960 het doctoraalexamen experimentele natuurkunde aflegde. De tentamina voor dit examen werden afgenomen door Prof.Dr. S.R. de Groot, Prof.Dr. P. Mazur en Prof.Dr. K.W. Taconis.

Van 1957-1960 werkte ik op het Kamerlingh Onneslaboratorium in de werkgroep voor molecuulphysica onder leiding van Prof.Dr. A.F. van Itterbeek (tot 1959) en Prof.Dr. K.W. Taconis. Eerst onderzocht ik samen met Drs. H. van Beelen de invloed van inwendige spanningen op het coërcitief veld van dunne ijzerlaagjes. Sinds begin 1958 assisteerde ik Dr. A.O. Rietveld bij zijn metingen van de viscositeit van mengsels van waterstofisotopen bij lage temperaturen en de thermodiffusie van H_2 - He en H_2 - D_2. Gedurende drie jaar was ik tevens als assistent verbonden aan het natuurkundig practicum voor precandidaten.

In september 1960 aanvaardde ik een werkkring als wetenschappelijk medewerker in gewoon verband aan het Laboratorium voor Massaspectrografie (nu F.O.M. - Instituut voor Atoom- en Molecuulfysica) te Amsterdam. Hier werkte ik aan de onderzoekingen die in dit proefschrift zijn beschreven.

In juli 1966 trad ik in dienst bij het Koninklijk Nederlands Meteorologisch Instituut te De Bilt, waarvan ik de directie mijn erkentelijkheid wil betuigen voor de medewerking die ik mocht ondervinden bij de voltooiing van dit proefschrift.

Graag wil ik van deze gelegenheid gebruik maken allen te bedanken die hebben bijgedragen aan de totstandkoming van dit proefschrift.

De plezierige samenwerking met Dr. J. Los, Dr. A.E. de Vries en Dr. D. Heymann zowel voor de technische als de meer fundamentele problemen, memoreer ik met vreugde. Prof.Dr. S.R. de Groot dank ik voor waardevolle suggesties.

I am greatly indebted to the management of the Dragon Project for giving me the opportunity during several symposia of seeing how the thermal diffusion column fits into the reactor plant as a whole. Dr. E. Römberg and the late Dr. H. de Bruijn particularly showed great interest in the experiments.

Alle medewerkers van de groep molecuulfysica hebben door raad en daad mij terzijde gestaan, speciaal H.W. Grotendorst en Mej. A. Tom, die met grote toewijding en nauwgezetheid een groot deel van het technisch werk en de metingen hebben verricht.

Bij de constructie van beide apparaten heb ik de hulp gehad van E. Keur, de werkplaats onder leiding van A.F. Neuteboom, de electronische afdeling onder leiding van P.J. van Deenen en de glasblazerij onder leiding van J.A. van Wel, die steeds voor alle moeilijkheden een oplossing wisten.

De heren G.J. de Ruyter en K. Vlam van de montage-afdeling van de Fa. Loos & Co N.V. ben ik dankbaar voor hun adviezen voor en testen van de hoge druk apparatuur.

De medewerking van Mej. M.J. Benavente (tekeningen), H. v.d. Brink (massaspectrometrische analyse), A. Haring (technische adviezen), F.L. Monterie en Th. van Dijk (fotografie), F. Vitalis (computerprogramma), Mej. J.M. de Vletter (typewerk) en A. Zwaal en J.C. Huyboom (vacuumtechniek) heb ik zeer op prijs gesteld.

CONTENTS

CHAPTER I

THEORY OF THE THERMAL DIFFUSION COLUMN

1. INTRODUCTION

The theory of thermal diffusion has been developed in a variety of books, papers and theses [2)17)18)19)20)]. Consider a binary gas mixture, subject to no external forces in which the pressure but not the temperature is uniform. Besides a heat flow there is also a diffusion flow. The equation of diffusion is given by:

$$\vec{J} = - \frac{p}{RT} \left[D_{12} \text{ grad } N - D_T \cdot \frac{1}{T} \text{ grad } T \right] \qquad (1.1)$$

where $\vec{J}$ is the flux density of the component, N its mole fraction, p the total pressure, T the temperature and R the gas constant per mole. D_T, which is named the thermal diffusion coefficient, gives the partial separation of the mixture as a consequence of the temperature gradient. D_{12} is the coefficient of ordinary concentration diffusion.

Usually D_T appears in the ratio D_T/D_{12}. This is called the thermal diffusion ratio and is denoted by K_T. As K_T is strongly dependent on the composition it is useful to introduce the thermal diffusion factor $\alpha = K_T/N\,(1 - N)$, which in general is independent of N.

Introducing this quantity (1.1) takes the following form:

$$\vec{J} = - \frac{p\, D_{12}}{R\, T} \left[\text{grad } N - \alpha N (1 - N) \text{ grad ln } T \right] . \qquad (1.2)$$

The thermal diffusion factor can be measured in two interconnected vessels, of which the upper one is kept at temperature T_2 and the lower one at T_1 ($T_2 > T_1$). The diffusion takes place in the connecting tube according to Eq. (1.2).

At the steady state $\vec{J} = 0$ and equation (1.2) can be integrated to yield

$$\ln Q = \int_{T_1}^{T_2} \alpha \, d \ln T \quad . \qquad (1.3)$$

The ratio $N_2/(1 - N_2)$ divided by $N_1/(1 - N_1)$ is called the separation factor Q, where N_2 is the concentration where the temperature is T_2 and N_1 the concentration where $T = T_1$.

As α is dependent on temperature and to a small degree on composition the integration of the right hand side of Eq. (1.3) gives only an average thermal diffusion factor $\overline{\alpha_T}$ for the temperature range T_1 to T_2 and the concentration range N_1 to N_2.

Disregarding dependence on concentration, which is allowed for trace components, with which the column experiments have been done, $\overline{\alpha}_T$ can be identified with the actual value of α at some average temperature $\overline{T}$ between T_1 and T_2 (Harrison Brown) [21].

The value of α at a definite temperature can be found from the slope of the curve ln Q versus ln T_2/T_1 by taking a series of measurements with the same value of T_1, but different values of T_2. Hence from Eq. (1.3):

$$\alpha = \frac{d \ln Q}{d \ln T_{2/T_1}} \quad . \tag{1.4}$$

α has to be taken positive if the lighter particle concentrates in the hotter part of the system.

2. THEORY OF THE THERMAL DIFFUSION COLUMN

The elementary effect in thermal diffusion processes can be multiplied by using convective motion of the gas. This is done in a thermal diffusion column, which essentially consists of two vertical surfaces, one kept at a higher temperature than the other. The gas mixture is now subjected to two effects: 1. thermal diffusion in the horizontal direction and 2. convective motion of the gas upwards near the hot wall and downwards near the cold one.

The theory of this countercurrent process has been given by different authors [20)22)23)]. The most elementary theory is that of K. Cohen [24)], considering the thermal diffusion column as a square cascade. Following his notation the column equation can be written as

$$c_6 \frac{\partial N}{\partial t} = c_5 \frac{\partial^2 N}{\partial z^2} - \frac{\partial}{\partial z} \left\{ PN + c_1 N(1 - N) \right\} \quad . \tag{1.5}$$

In this equation c_1 is the column parameter representing the axial transport of the desired component under the influence of the radial separating mechanism and the axial flow. This is counter-balanced by the axial back diffusion on one side and the disturbance in the radial diffusion stream caused by the axial countercurrent on the other side. These two terms are represented in c_5. The product stream of the column is P, the hold-up per cm length is represented by c_6, z is the vertical coordinate and t the time.

For the integration of (1.5) we make use of Cohen's equation (1.82) (p. 28) $\partial \tau / \partial z = - c_6 \, \partial N / \partial t$, where the amount of desired isotope flowing through a cross section of the column per unit of time is denoted by τ. In the steady state τ is no longer a function of z and consequently it equals PN_p, where N_p is the mole fraction

of the product. The result of the integration is:

$$\tau = PN + c_1 N(1 - N) - c_5 \frac{\partial N}{\partial z} \quad . \tag{1.6}$$

For a column operated at total reflux, that is with zero production rate,

$$\tau = c_1 N(1 - N) - c_5 \frac{\partial N}{\partial z} \quad . \tag{1.7}$$

A. The column parameters

The column parameters c_1 to c_6 are different for different types of columns, such as for:

1. Plane parallel plates
2. Concentric cylinders
3. "Hot wire" type.

They can be calculated from a set of equations. For the plane parallel plates the equations are given in cartesian coordinates, for the cylindrical types in cylindrical coordinates.

According to Cohen the parameters are then given by:

Cartesian coordinates	Cylindrical coordinates
$c_1 = - B \int_0^d \alpha \frac{\partial \ln T}{\partial x} dx \int_0^x \rho v dx$	$c_1 = - 2\pi \int_{r_h}^{r_c} \alpha \frac{\partial \ln T}{\partial r} dr \int_{r_h}^{r} \rho v r dr$
$c_2 = B \int_0^d \rho D dx$	$c_2 = 2\pi \int_{r_h}^{r_c} \rho D r dr$
$c_3 = B \int_0^d \frac{dx}{\rho D} \left[\int_0^x \rho v dx \right]^2$	$c_3 = 2\pi \int_{r_h}^{r_c} \frac{dr}{\rho D r} \left[\int_{r_h}^{r} \rho v r dr \right]^2$
$c_5 = c_2 + c_3$	$c_5 = c_2 + c_3$
$c_6 = B \int_0^d \rho dx$	$c_6 = 2\pi \int_{r_h}^{r_c} \rho r dr$
$P = B \int_0^d \rho v dx$	$P = 2\pi \int_{r_h}^{r_c} \rho v r dr$

where: r is the radial and x the horizontal coordinate,
r_c is the radius of the cold cylinder (cm),
r_h is the radius of the hot cylinder (cm),
ρ is the total density of the gas mixture (g cm^{-3}),
v is the convection velocity in axial direction,
d is the distance between hot wall and cold wall.

For the nearly plane case of the concentric cylinder column the integrals can be simplified by substituting for r the mean value $\frac{1}{2}(r_c + r_h)$. The column parameters then reduce to the parallel plates case, where B has to be replaced by $\pi(r_c + r_h)$ and d by $r_c - r_h$.

Different authors have given expressions for the column parameters (Jones and Furry [22], Fleischmann and Jensen [23], Slieker [25]) assuming that the temperature difference ΔT is small.

For the plane parallel plates the results of Jones and Furry, Fleischmann and Jensen, and Slieker agree in all respects. The temperatures of the walls are T_1 and T_2; $T_2 - T_1 = \Delta T$. The transport coefficients of the gas, namely the coefficient of viscosity η, the coefficient of thermal conductivity λ, the thermal diffusion factor α and the diffusion coefficient D and the density ρ occurring in the formulas, are taken at the mean temperature $\overline{T} = (T_1 + T_2)/2$.

The column parameters are:

$$c_1 = \frac{d^3 \rho^2 \alpha g}{6 ! \eta} B \left(\frac{\Delta T}{\overline{T}}\right)^2 \tag{1.8}$$

verse fifth power of the distance.

$$c_2 = \rho D d B \tag{1.9}$$

$$c_3 = \frac{d^7 \rho^3 g^2}{9 ! \eta^2 D} B \left(\frac{\Delta T}{\overline{T}}\right)^2 \tag{1.10}$$

where Table I.1 gives the conversion between the symbols used by the different authors.

The experiments described in this thesis have been done with a concentric cylinder column. Unfortunately the theory is very complicated, so that several approximations have been made.

Jones and Furry derive an equation with the assumptions that ΔT is small, $r_c/r_h < 2.7$ and the molecules repel one another with a force that varies as the inverse fifth power of the distance.

The derivation made by Slieker is based on a cylindrical differential equation where he takes the temperature dependent quantities at the mean temperature

$$\overline{T} = T_1 + \Delta T \frac{0.56}{\ln r_c/r_h} \tag{1.11}$$

instead of introducing a molecular model, which takes into account the temperature dependence of the transport coefficients.

TABLE I.1

Comparison of symbols used by Jones and Furry, Fleischmann and Jensen and Slieker

	Jones/Furry	Fleischmann	Slieker
transport factor	H	τ_o	c_1
axial back diffusion	K_d	-	c_2
losses due to axial countercurrent	K_c	-	c_3
total effects $c_2 + c_3$	K	$\tau_o L$	c_5
mass of gas per cm column	μ	-	c_6
characteristic length	1/2 A	L	c_5/c_1
half "Trennschärfe"	A	1/2 L	ε
equilibrium separation factor	$q_e = e^{2AL}$	$A = e^{Z/L}$	$q = e^{2\varepsilon Z}$
length of column	L	Z	Z
distance between the walls	2 w	Δ x	d
mean circumference	B	U	B
radius of outer tube	r_1	R_a	r_c
radius of inner tube	r_2	R_i	r_H
mole fraction	c	c	N
mass of gas in $^+$ve reservoir	m^+	M	H
pressure	P	p	p
production rate	σ	G	P

Fleischmann and Jensen give only formulas for the hot wire model. They, however, extrapolate their results to the concentric cylinder model graphically.

We shall now compare the three authors' expressions for c_1 and c_5 with the parallel plate model. In the concentric cylinder column we have to write $\pi(r_c + r_h)$ instead of B and $r_c - r_h$ instead of d in Eq. (1.8), (1.9) and (1.10). Then, substituting $a = r_h/r_c$ these equations can be written as:

$$c_1 = \pi (1-a)^2 (1-a^2) \frac{r_c^4 \rho^2 g \alpha}{6 : \eta} \left\{\frac{\Delta T}{\bar{T}}\right\}^2 = P_1 \frac{r_c^4 \rho^2 \alpha g}{6 : \eta} \left\{\frac{\Delta T}{\bar{T}}\right\}^2$$

$$c_2 = \pi (1-a^2) r_c^2 \rho D = P_2 r_c^2 \rho D$$

$$c_3 = \pi (1-a)^6 (1-a^2) \frac{r_c^8 \rho^3 g^2}{9 : \eta^2 D} \left\{\frac{\Delta T}{\bar{T}}\right\}^2 = P_3 \frac{r_c^8 \rho^3 g^2}{9 : \eta^2 D} \left\{\frac{\Delta T}{\bar{T}}\right\}^2$$

In the same way the last two factors can be split off from Jones', Fleischmann's and Slieker's equations, hence:

Jones and Furry:

$$c_1 = J_1 P_1 \frac{r_c^4 \rho^2 \alpha g}{6 : \eta} \left\{\frac{\Delta T}{\bar{T}}\right\}^2 \qquad c_2 = J_2 P_2 r_c^2 \rho D$$

$$c_3 = J_3 P_3 \frac{r_c^8 \rho^3 g^2}{9 : \eta^2 D} \left\{\frac{\Delta T}{\bar{T}}\right\}^2$$

Fleischmann and Jensen:

$$c_1 = F_1 P_1 \frac{r_c^4 \rho^2 \alpha g}{6 : \eta} \left\{\frac{\Delta T}{\bar{T}}\right\}^2 \qquad c_2 = F_2 P_2 r_c^2 \rho D$$

$$c_3 = F_3 P_3 \frac{r_c^8 \rho^3 g^2}{9 : \eta^2 D} \left\{\frac{\Delta T}{\bar{T}}\right\}^2$$

Slieker:

$$c_1 = [S.F.]_1 \frac{r_c^4 \rho^2 \alpha g}{6 : \eta} \left\{\frac{\Delta T}{\bar{T}}\right\}^2 \qquad c_2 = P_2 r_c^2 \rho D$$

$$c_3 = [S.F.]_3 \frac{r_c^8 \rho^3 g^2}{9 : \eta^2 D} \left\{\frac{\Delta T}{\bar{T}}\right\}^2$$

where J_1, J_2 and J_3 are infinite series in $\Delta T/2\overline{T}$ and $\ln r_c/r_h$, as Jones' correction on the plane parallel plates type;
where F_1, F_2 and F_3 can be interpolated from Fig. 8 in Fleischmann's article, but not very accurately;
where $[S.F.]_1$ and $[S.F.]_3$ are tabulated as a function of r_c/r_h in Slieker's article [25].

We apply this to a column for which $T_1 = 20\ ^{\circ}C$, $T_2 = 360\ ^{\circ}C$, $r_c = 10$ mm and $r_h = 4$, 5, 6.7 or 8.3 mm.

The result is given in Table I.2.

TABLE I.2

Calculated values for the same constant in the column parameters c_1, c_2 and c_3 for concentric cylinder columns according to different authors and compared with values for the plane parallel plates.

Column param.	a	a^{-1}	Jones & Furry J.P.	Fleischmann F.P.	Slieker [S.F.]	Parallel plates P
c_1	0.40	2.50	1.2033	0.7716	0.8274	0.9500
	0.50	2.00	0.7185	0.5035	0.5433	0.5890
	0.67	1.50	0.2218	0.1768	0.1885	0.1939
	0.83	1.20	0.0287	0.0257	0.0259	0.0267
c_2	0.40	2.50	0.7842	0.8336	0.8400	0.8400
	0.50	2.00	0.7208	0.7378	0.7500	0.7500
	0.67	1.50	0.5535	0.5419	0.5556	0.5556
	0.83	1.20	0.3127	0.3016	0.3056	0.3056
c_3	0.40	2.50	0.1933	0.0901	0.1042	0.1231
	0.50	2.00	0.0527	0.0286	0.0334	0.0368
	0.67	1.50	$0.3004.10^{-2}$	$0.2025.10^{-2}$	$0.2302.10^{-2}$	$0.2394.10^{-2}$
	0.83	1.20	$0.2294.10^{-4}$	$0.1918.10^{-4}$	$0.1956.10^{-4}$	$0.2058.10^{-4}$

The greatest difference between the last column and Slieker's values is 10%. So the formulas for the parallel plates can be used to design the column described in Chapter II. The most striking point, however, is the fact that Jones and Furry's shape factors, which are temperature dependent, are larger than the parallel plate type in contrast with those of the other authors.

B. The steady state and the equilibrium time

When the column starts to work the concentration gradient is zero everywhere in the column, so (1.7) leads to:

$$(\tau)_{t=o} = c_1 N(1 - N) \tag{1.12}$$

being the initial transport.

For a column working at total reflux we start with Eq. (1.7) to calculate the stationary state separation. In the steady state where the concentrations in the reservoirs and in the column are independent of time, the net transport has become zero, so $c_1 N(1 - N) = c_5 \partial N/\partial z$. This can be integrated for a column of length Z. The separation

$$Q = \frac{N_z}{1 - N_z} \cdot \frac{1 - N_o}{N_o}$$

is given by

$$\ln Q = \frac{c_1}{c_5} Z \tag{1.13}$$

or $$Q = e^{2\varepsilon Z}$$

with $$\varepsilon = c_1/2c_5$$

where N_z is the mole fraction of the component at the place where it concentrates and N_o is the mole fraction of the same component at the other end of the column.

Introducing (1.8), (1.9) and (1.10), (1.13) becomes:

$$\ln Q = Z \frac{\frac{d^3 \rho^2 \alpha g}{6 ! \eta} \left(\frac{\Delta T}{\overline{T}}\right)^2}{\rho D d + \frac{d^7 \rho^3 g^2}{9 ! \eta^2 D} \left(\frac{\Delta T}{\overline{T}}\right)^2} = 0.837 \frac{Z}{d} \alpha \frac{\Delta T}{\overline{T}} \frac{m}{1 + m^2} \tag{1.14}$$

where $$m = \frac{d^3 \rho g \Delta T}{602.4 \eta D \overline{T}} \tag{1.15}$$

If we assume η independent of the pressure, $\rho \propto p$ and $D \propto p^{-1}$, then $m \propto p^2$. From Eq. (1.14) it follows because α is independent of pressure that ln Q is only a function of the density through m. Hence ln Q is a maximum when m = 1 and we can define the optimum pressure p_{opt} as:

$$p^2_{opt} = 602.4\ p_o^2\ \frac{\eta D_o \bar{T}}{d^3 \rho_o g \Delta T} \qquad (1.16)$$

and $$m = \frac{p^2}{p^2_{opt}} \qquad (1.17)$$

where the index $_o$ means that the value has to be taken at some reference pressure p_o.

m can be introduced in Eq. (1.8) leading to

$$c_1 = 0.837\ \rho D \alpha\ \frac{\Delta T}{\bar{T}}\ B\ m. \qquad (1.18)$$

In the general case the stationary state separation factor can be found from equation (1.6), substituting for τ the net production rate $P N_p$.

$$P N_p = PN + c_1 N(1 - N) - c_5 \frac{\partial N}{\partial z} \qquad (1.19)$$

Integration with the boundary conditions $N = N_o$ at $z = 0$ (upper side of the column) and $N_z = N_p$ at the bottom side of the colomn, gives

$$Z = \frac{1}{\varepsilon \Delta(\psi)}\ \tanh^{-1}\ \frac{(N_p - N_o)\ \Delta(\psi)}{(N_p - 2N_p N_o + N_o) - (N_p - N_o)\psi} \qquad (1.20)$$

where $\psi = P/c_1$ is the normalized production rate

and $\Delta(\psi) = \sqrt{1 + 2\psi(1 - 2N_p) + \psi^2}$.

When $N_o \ll 1$ and $N_p \ll 1$, $\Delta(\psi) = 1 + \psi$ and Eq. (1.20) takes the simpler form:

$$Z = \frac{1}{2\varepsilon(1 + \psi)}\ \ln\ \frac{N_p}{N_o - \psi(N_p - N_o)}$$

Hence the enrichment of a trace component in the product stream as compared with the initial concentration is:

$$\frac{N_p}{N_o} = Q = \frac{(1 + \psi)\, e^{2\varepsilon Z (1 + \psi)}}{1 + \psi\, e^{2\varepsilon Z (1 + \psi)}} \qquad (1.21)$$

Fleischmann and Jensen, in their article [23], give

$$G = \frac{\tau}{c_z - c_o}$$

where G is the production rate. Using their formula (23 a)

$$\frac{\tau}{\tau_o} = c_o \frac{A - a}{A - 1},$$

where A is the equilibrium separation for a column at total reflux and $a = c_z/c_o$ we get

$$G = \tau_o \frac{A - a}{(a - 1)(A - 1)} .$$

With Table I.1 this can be translated into Cohen's notation:

$$\frac{G}{\tau_o} = \frac{P}{c_1} = \psi = \frac{e^{2\varepsilon Z} - \frac{N_p}{N_o}}{\frac{N}{(\frac{p}{N_o} - 1)(e^{2\varepsilon Z} - 1)}}$$

or $$\frac{N_p}{N_o} = \frac{(1 + \psi) e^{2\varepsilon Z}}{1 + \psi e^{2\varepsilon Z}} .$$

It can be seen that Fleischmann's formula is the same as Cohen's, when the product P or $\psi \ll 1$.

The equilibrium time of a thermal diffusion column can be found by solving Eq. (1.5) or (1.6). The boundary conditions are determined by the mode of operation. There are different types of operation: with or without production, with finite reservoirs no reservoirs or with an infinite upper reservoir, which means that at the negative end of the column the concentration N_o is kept constant, for example by flushing it with fresh mixture.

In one method of operation we kept the concentration of the trace component at the top of the column constant. This case could be approximated by the derivation of Jones and Furry, who considered this system, assuming that the harmonic mean of the volumes of the reservoirs is large as compared with the volume of the column, for $N \ll 1$. The significance of this assumption is that τ is independent of z and depends only on the time t.

Assuming that the reservoir at the positive end contains a quantity of H(gramme) we can give the time variation of N_z by

$$\frac{dN_z}{dt} = \frac{\tau}{H} \tag{1.22}$$

The concentration at the negative end remains N_o. The time required for the concentration in the positive reservoir to rise from N_o to N is given by

$$t_{(N)} = H \int_{N_o}^{N} \frac{dN_z}{\tau} \quad . \tag{1.23}$$

When N is everywhere much less than unity, Eq. (1.7) becomes

$$\tau = c_1 N - c_5 \frac{\partial N}{\partial z} \quad .$$

This can be integrated with the boundary conditions that $N = N_o$ for $z = 0$ and $N = N_z$ for $z = Z$. The result is

$$\frac{\tau}{c_1} = N_o \frac{Q - q}{Q - 1} \tag{1.24}$$

with $Q = e^{c_1 Z / c_5}$ and $q = \frac{N_z}{N_o}$. (1.25)

Introducing (1.24) in (1.23) gives

$$\frac{Q - q}{Q - 1} = e^{-t/t_r} \tag{1.26}$$

with the relaxation time $t_r = \frac{H}{c_1} (Q - 1)$. (1.27)

(1.26) represents an exponential approach to equilibrium with t_r being the time to reach $(e - 1)/e = 63.2\%$ of the equilibrium separation Q.

In another method of operation we had a very large but finite negative upper reservoir. The formula of Jones and Furry can be extended for this case in the following way:

Suppose the negative reservoir contains a mass H' (gramme)

$$\frac{dN_o}{dt} = -\frac{\tau}{H'} \quad .$$

With Eq. (1.22) and (1.25)

$$\frac{\tau}{H} = \frac{dN_z}{dt} = \frac{d\,q\,N_o}{dt} = N_o \frac{dq}{dt} + q \frac{dN_o}{dt} = N_o \frac{dq}{dt} - q \frac{\tau}{H'}$$

or $$N_o \frac{dq}{dt} = \frac{\tau}{H} + \frac{q\tau}{H'} \tag{1.28}$$

and then from (1.24)

$$\frac{dq}{dt} = c_1 \frac{Q - q}{Q - 1} \left\{ \frac{1}{H} + \frac{q}{H'} \right\}$$

which can be integrated, giving

$$\frac{(Q - q)\ (1 + H'/H)}{(Q - 1)\ (q + H'/H)} = e^{-t/t_r} \tag{1.29}$$

where

$$t_r = \frac{Q - 1}{c_1 \left(\frac{Q}{H'} + \frac{1}{H}\right)} \tag{1.30}$$

which has, however, not such a definite meaning as in (1.27). For $H' \longrightarrow \infty$ this equation is the same as (1.26).

C. Limitations of the theory

For the theory developed above it is assumed that there is a non-turbulent convective flow in the column. The dimensionless number, used in problems on free convection, upon which the action of a thermal diffusion column is essentially based, is the Grashof - Prandtl number:

$$Gr\ Pr = \frac{\rho^2\ g\ d^3\ \Delta T\ c_p}{\eta\ \lambda\ \bar{T}} \tag{1.31}$$

with c_p being the heat capacity at constant pressure.

The heat conductivity between two vertical or horizontal plates as a function of Gr Pr has been investigated by several people, e.g. Gröber, Erk, Grigull [26], Beckmann [27], Sellschopp [28]. From these experiments it follows that a laminar current is developed only when Gr Pr > 1700.

The turbulence starts when Gr Pr > 10^6, according to experiments of Krausold [29].

In literature on thermal diffusion there are only a few remarks regarding this

flow number. They are generally expressed in the Reynolds number

$$Re = \frac{\rho^2 \, g \, d^3 \, \Delta T}{384 \, \eta^2 \, \bar{T}} \qquad (1.32)$$

From (1.31) it follows that $Gr\ Pr = \frac{c_p \eta}{\lambda} \cdot 384\ Re$, where $Pr = \frac{c_p \eta}{\lambda}$ the Prandtl number is 0.70 for helium.

The condition for laminar flow is then

$$6.3 < Re < 3720.$$

Onsager and Watson [30] have shown experimentally that turbulence starts when $Re > 25$. Donaldson and Watson [31] found that laminar flow breaks down for $Re = 14$. Jones and Furry [22] stated $Re = 10$ as the maximum permissible value of Re.

Grew and Ibbs [2] state that the spacing d in a thermal diffusion column should be adjusted so that $5 < c_3/c_2 < 25$. This relation can be transformed with Eq. (1.9) and (1.10). For a pure gas or a mixture of isotopes the result is $4.7 < Re < 10.5$. Use has been made of the relation

$$D = \frac{6}{5} A^* \eta/\rho$$

with $A^* \approx 1.1$, the quotient of two collision cross sections

$$\Omega^{(2,2)*} / \Omega^{(1,1)*}.$$

Summarizing the condition for laminar flow in a thermal diffusion column can be given as

$$5 < Re < 10 \quad . \qquad (1.33)$$

This limitation means that the working pressure may be far off the optimal pressure.

From experiments by Saxena and Mason [32] on diffusion of trace components CO_2 in He it follows that $\rho D_{12}/\eta = 0.50$. Using this and Eq. (1.15), (1.17) and (1.32)

$$Re = 0.78\ m \quad . \qquad (1.34)$$

The condition for laminar flow becomes

$$6.4 < m < 12.8$$

or $$2.5\ p_{opt.} < p < 3.6\ p_{opt.}$$

The integration of the formulas has been done by assuming that the density and the transport coefficients do not vary over the radius of the column. Values of the different constants are taken at the mean temperature $\overline{T}$ given by

$$\overline{T} = T_1 + \frac{0.56}{\ln r_c/r_h} \Delta T$$

according to the formula of Fleischmann and Jensen [23], which means that $\overline{T}$ is taken as the temperature corresponding to the point, where the convection current changes sign.

The concentration dependence of η, ρ, λ and D has not been taken into account either; this is admissible because the experiments have been done with one of the components in trace concentration.

In the derivation of the formulas also the quasistationary state assumption and the assumption that the temperature distribution is determined by conduction alone are used. These approximations, however, do not show the most serious deviations between experiment and theory. They are caused by imperfection in the thermal diffusion column, such as variations in the diameter of the tubes and parasitic convection currents due to temperature gradients in axial and azimuthal direction. The effect of these factors is that the result of the experiment is lower than theory predicts. These irregularities can be given in the formulas by adding another cascade parameter c_7 or K_p to c_2 and c_3 (Dickel [33) 34)]).

CHAPTER II

THERMAL DIFFUSION COLUMN: EXPERIMENTS

1. DESIGN AND CONSTRUCTION OF THE THERMAL DIFFUSION COLUMN

The purpose of the column was to concentrate trace quantities of CO_2 in helium at 20 atm pressure with a factor hundred in as short a time possible. Owing to these special requirements a concentric cylinder type thermal diffusion column was built. The most outstanding advantage of a concentric cylinder column is that it can be constructed very firmly, which is especially important when the column has to work for a long period and when there is no opportunity for repairs. Moreover, the value of c_1 can be made very high for a fixed value of the gap d, which is important for short relaxation times. The inner cylinder can be made of a good heat conductor, thus preventing temperature gradients in axial and azimuthal direction. Disadvantages of this type of column are that its construction requires high precision and it consumes more power per unit length than the hot-wire column.

The dimensions of the column were calculated in the following way:

When a temperature difference of 260° and a mean temperature of 420 °K is assumed, then according to Eq. (1.33) the gap d should be between 3.2 and 4.2 mm. As 20 mm seemed a convenient diameter for the outer tube, heating rods with a diameter of 12 or 13 mm would fulfil the requirements set by the Reynolds number. The separation in the column is given by (1.14). At the working point Re = 6.0 and with (1.34) m = 7.7. When α is taken from the experiments described in chapter IV as 0.916, $\ln Q = 0.173\ Z$. For a column length of 100 cm $\ln Q = 17.3$. So theoretical enrichments of $Q = 32.6 \times 10^6$ could be expected. The dimensions were calculated on the high side to keep the relaxation time for Q = 100 short. Besides that it is better to work in the linear part of the ln Q versus time graph, where the results reproduce better than at equilibrium, according to experiments by Dickel [33) 34)].

A. Construction

The thermal diffusion column consists of three concentric stainless steel tubes. The outer two tubes together form the cooling water jacket W. Special attention was paid to the straightness of the inner tube, because this forms the boundary of the thermal diffusion region D. For this purpose first the outer tube was welded into the unmachined end flanges F, then the flanges were squared on the tube and turned off parallel to each other on a lathe. Finally the inner tube was welded into the end flanges at a temperature which was about 50 °C higher than the outer one. Under normal operating condition the pipe was then stretched by tensile force.

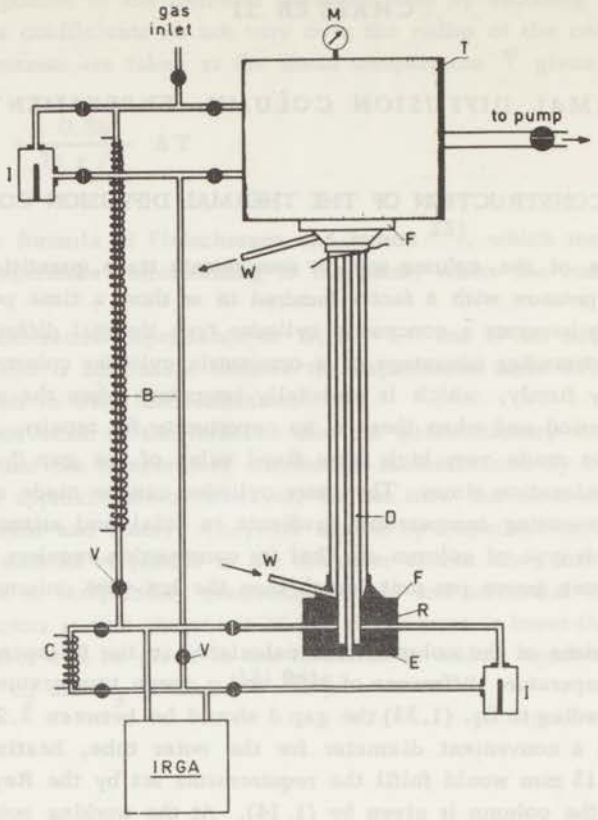

Fig. 1

Scheme of the thermal diffusion column with auxiliary equipment. Explanation in the text.

For the hot tube we chose different diameters in order to determine experimentally the best possible gap width. This tube was closed at the upper end and welded into a flange E at the lower end so that it could be exchanged easily. Triangle-shaped spacers were soldered vertically to the tube 120° apart at intervals of 20 cm. Fig. 1 shows the construction of the column with upper and lower reservoir and connecting pipes.

The heater inside was a Kanthal A - 1 wire (diam. 1.5 mm) *), insulated with aluminium oxide. The space between heating wire and tube wall was filled with copper to ensure symmetrical temperature distribution over the surface of the tube. The maximum possible heat input over the entire tube length was about 2 kW.

*) A.B. Kanthal, Hallstahammar, Sweden.

Temperature measurements were taken with a chromel-alumel thermocouple soldered inside the stainless steel tube. The temperature difference could also be calculated from the heat input E as

$$\Delta T = \frac{E}{2 \pi \lambda Z} \ln r_c / r_h \qquad (2.1)$$

where λ is the coefficient of conducting of heat.

The column formed the connection between two reservoirs. The upper reservoir T, with a volume of 20,000 cc, was large in comparison with the volume of the column and lower reservoir; this was to keep the CO_2 concentration as constant as possible. In the case of large separations, however, there was still a depletion of impurity concentration. Therefore, in some experiments the CO_2 concentration in the upper volume was kept at the initial value by connecting a small reservoir with $MgCO_3$. The reservoir was kept at a constant temperature by means of a thermostat, resulting in a constant vapour pressure of CO_2.

The lower reservoir R was made as small as possible in order to get the lowest relaxation time in the apparatus. It consisted of the analysing instruments (infra-red gas analyser or ionization chamber I) and connecting pipes. Convective action by heating one of the vertical pipes C was used for recycling: the time for one cycle, being about 10 minutes, is short compared with the relaxation time of the column. Consequently the CO_2 concentration at the bottom could be followed continuously.

The pressure of the gas in the column was read from a Bourdon manometer M.

A double by-pass B was included, connecting upper and lower reservoirs. Thus it is possible to measure the concentration in the upper reservoir and to remix the contents after each run.

The dimensions of the column were:

upper volume	20,000 cc
lower volume	80 to 170 cc
outer radius cooling jacket	1.6 cm
inner radius cooling jacket	1.0 cm
radius heating cylinder	0.6, 0. 65, 0.7 cm
length of column	100 cm

B. The analysis instruments

Originally the measurements of the CO_2 concentration were made with an infra-red gas analyser (I.R.G.A., SB 2, Grubb Parsons, New Castle, U.K.). In this instrument two parallel beams of infra-red radiation produced by the nichrome heater A are reflected simultaneously through two absorption tubes B. One is filled with the mixture to be analysed, so that absorption occurs. The other one is sealed off. Both beams are absorbed in the two vessels C, which are filled with the gas to be detected

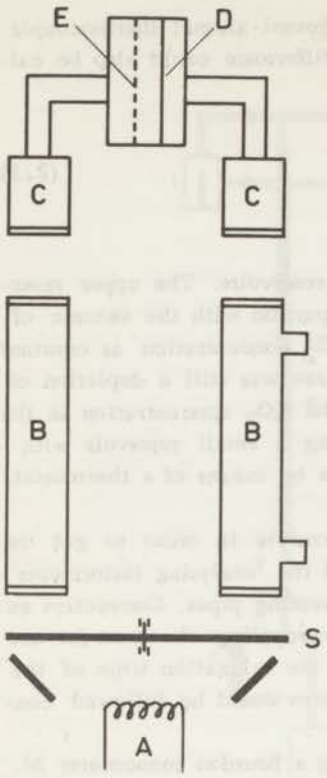

Fig. 2
Diagram of the infra-red gas analyser.
A. heater
B. absorption tube
C. detector
D. metal diaphragm
E. perforated metal plate

in pure form. The infra-red light produces a heating effect in C which results in a pressure difference on the thin metal diaphragm D. With an adjacent insulated and perforated metal plate E this forms an electrical condensor. The beams are operated intermittently by menas of a rotating shutter S and the capacity changes are amplified and registered (Fig. 2).

However, this apparatus has a few disadvantages. The I.R.G.A. used had an absorption tube divided into three parts with lengths 1 : 10 : 100 to extend the concentration range to be measured. The length of the absorption tube to be used depends on the concentration range to be covered. The guiding rule is that concentration times length should be approximately constant. However, at high pressures it is difficult to change over from one tube to another during a measurement, because the parts not in use have to be flushed with CO_2 - free helium of 20 atm. In this case, therefore, the concentration range to be measured is only factor 50, as it is limited at low readings by the zero drift and at high concentrations by the departure from linearity.

In the second place the I.R.G.A. reading showed a discontinuity at 3 atm, probably owing to deformation of the windows and is therefore not reproducible.

As it was also difficult to measure upper and lower concentration with only one I.R.G.A., in later experiments ionization chambers were used. They are discussed in chapter IV.

2. EXPERIMENTS

The column was evacuated with a rotating pump and an oil diffusion pump to a pressure of 10^{-5} Torr and the inner cylinder and other parts of the apparatus were heated. When the system was vacuumtight the CO_2 was introduced. It was found that part of the CO_2 adsorbed on the walls. The reading on the infra-red gas analyser showed that about 2 cc N.T.P. was adsorbed.

After the CO_2 the carrier gas, commercial tank helium, was introduced. It was passed slowly over a charcoal trap at liquid air temperature.

The gas was thoroughly mixed by convective action through a by-pass until an adsorption equilibrium was reached. The CO_2 molecules on the heating rod desorbed from it when the current was switched on, giving flattered enrichments. Therefore, the heating cylinder was already at the desired temperature during mixing and the experiment was started up by closing the valves V in the by-pass (Fig. 1).

A. Preliminary experiments

In the first experiments only the change in concentration of CO_2 in the lower volume was measured. The CO_2 concentration in the upper volume was calculated from the ratio of both volumes (mass balance). This method is dependent on desorption and adsorption phenomena. Therefore, the CO_2 concentration at the top was measured at the end of an experiment. The difficulty was that two quite different concentrations had to be measured with only one I.R.G.A. Hence the absorption tube first had to be flushed with pure helium at 20 atm by means of two reducing valves until the reading was zero again.

These experiments showed that the mass balance was violated. It was found that the enrichment measured at the bottom was much too low owing to adsorption of CO_2 on the walls and the non-linearity of the I.R.G.A. reading.

In other experiments the CO_2 concentration at the top of the column was kept constant in order to have an infinite upper reservoir and to simulate the conditions in the reactor, where a constant flow of helium with CO_2 passes along the top of the column.

A little reservoir with granulated $MgCO_3$ was connected with the upper reservoir. Table II.1 shows that the CO_2 concentration in the top of the column could be kept constant in a large range from 1 to 50 p.p.m. by taking a temperature between 137° and 200 °C.

TABLE II.1

CO_2 pressure of $MgCO_3$ at different temperature [35].

t (°C)	p_{CO_2} (atm)	CO_2 concentration at 20 atm He
137	1.49×10^{-5}	0.7 p.p.m.
157	6.67×10^{-5}	3.3 "
177	2.61×10^{-4}	13 "
197	9.08×10^{-4}	45 "

The initial CO_2 concentration was 1 p.p.m. The thermostat was therefore adjusted to $140 \pm 0.5\ ^{o}C$.

The experiments were carried out with heating cylinders of 12 and 13 mm diameter. The volume of the lower reservoir was 80 cc.

As stated in Section 1B of this chapter the enrichment that could be measured in the I.R.G.A. was only a factor 50. The results are therefore only reliable up to q = 50; above this value there is a large discrepancy between theory and experiment.

It was possible on the other hand to compare the initial transport with theory. This is done in Table II.2.

TABLE II.2

Initial transport, Reynolds numbers and the time taken to reach q = 50 for two columns with $H' = \infty$.

diameter heating rod (mm)	temperature heating rod (^{o}C)	Reynolds number Re	exp. transp. / theor. transp.	q = 50 after	
13	158	6.4	0.66	4.2 hours	
"	273	6.1	0.74	2.0 "	
"	419	4.8	0.88	1.1 "	
12	177	9.6	0.79	7.8 "	*)
"	265	9.1	0.72	2.3 "	
"	303	8.7	0.91	1.2 "	

*) this experiment was carried out with a lower volume of 170 cc.

The initial transport is given by Eq. (1.12).

When the hold-up of the column itself can be ignored as compared with the hold-up H of the lower reservoir, and the upper reservoir is taken as infinite, the relation $H\ \partial N/\partial t = c_1 N(1 - N)$ holds. For $N \ll 1$ this equation can be integrated:

$$\ln \frac{N_t}{N_o} = \ln q = \frac{c_1}{H} t \quad ,$$

where N_t is the concentration after time t. For very short times, when $N_t - N_o \ll N_o$:

$$\frac{N_t - N_o}{N_o} = \frac{c_1 t}{H} \qquad (2.2)$$

The slope of the separation curve as a function of time yields the transport factor c_1.

It turned out experimentally that the rise in concentration was linear with time, but it was dependent on the velocity of the recycling to the effect that oscillations occurred when the speed was less than 6.5 cc/min as shown in Fig. 3 a.

When the velocity of the recycling rose above 6.5 cc/min the oscillations gradually disappeared and the separation curve became a straight line (Fig. 3 b). It was found that when in the first case for H the hold-up of the analysing cell had been taken and in the second case the hold-up of the whole lower reservoir, the c_1's calculated in this manner agree.

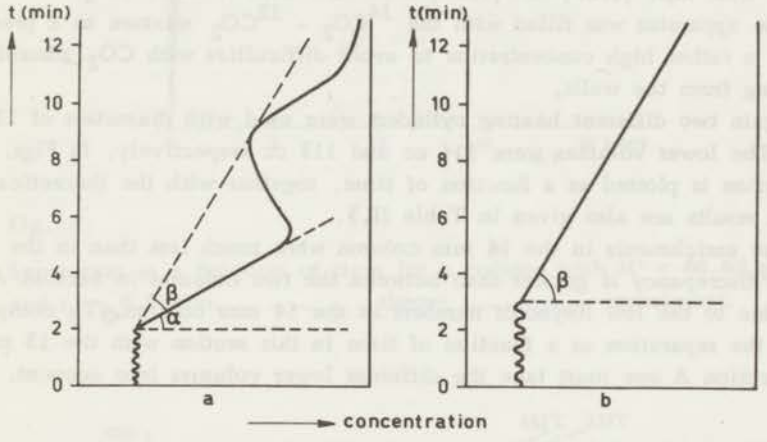

Fig. 3

Reproduction of two recorder charts of a separation of $^{14}CO_2$ - He in the column.

At a lower velocity the enriched gas first filled the analysing cell and adsorbed on the wall; at high velocities it passed the cell as a jet.

It must be pointed out here that Eqs. (1.26) and (1.27) give a different result for large Q's. The time taken to reach separation q is here

$$\frac{Q - q}{Q} = e^{-t/t_r} \qquad \text{with} \qquad t_r = \frac{HQ}{c_1}$$

$$\ln (1 - q/Q) = -q/Q = -\frac{tc_1}{HQ} \qquad t = \frac{Hq}{c_1} \tag{2.3}$$

This formula cannot be valid for $t = 0$.

B. Experiments with ionization chambers

For the reasons discussed above (II.1B) and in order to be able to work with higher initial concentrations of CO_2 in two analysing instruments, ionization chambers were used in the new experiments.

The experiments were carried out with a $^{14}CO_2$ - $^{12}CO_2$ mixture as impurity. An ionization chamber was connected with the upper reservoir as well as with the lower reservoir, so that the separation $Q = N_{lower}/N_{upper}$ could be measured continuously. It was impossible to use a homogeneous $Mg^{14}CO_3$ - $Mg^{12}CO_3$ mixture to ensure a constant $^{14}CO_2$ concentration at the top as discussed in Section A. For the relaxation time Eqs. (1.29) and (1.30) were used with H' = 66.68 g.

The apparatus was filled with the $^{14}CO_2$ - $^{12}CO_2$ mixture to a pressure of 2.5 Torr, a rather high concentration to avoid difficulties with CO_2 adsorbing on to or desorbing from the walls.

Again two different heating cylinders were used with diameters of 13 and 14 mm. The lower volumes were 114 cc and 113 cc respectively. In Figs. 4 and 5 the separation is plotted as a function of time, together with the theoretical separation. The results are also given in Table II.3.

The enrichments in the 14 mm column were much less than in the 13 mm one. The discrepancy is greater than between the two columns in Section A. This must be due to the low Reynolds numbers in the 14 mm column. To compare the results of the separation as a function of time in this section with the 13 mm column of Section A one must take the different lower volumes into account.

TABLE II.3

Initial transport and separation factors as a function of time for two columns with H' = 66.68 g.

diameter heating rod (mm)	temperature heating rod (°C)	Reynolds number Re	exp. transp. / theor. transp.	q = 100 after	separation after		
					5 hrs	10 hrs	15 hrs
13	157	6.4	0.71	7.7 h.	59	141	242
"	280	6.1	0.56	6.5 h.	69	180	331
"	298	5.9	0.80	5.0 h.	101	247	463
14	180	4.0	0.67	20.5 h.	26	53	78
"	331	3.5	0.50	11.5 h.	35	83	143
"	453	2.8	0.49	11.0 h.	38	88	152

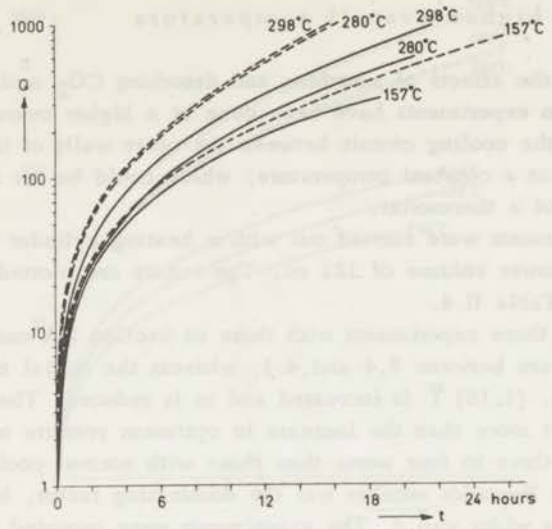

Fig. 4

Separation as a function of time for a column with H' = 66.68 g and r_h = 6.5 mm. – – – – – theory ———— experiment.

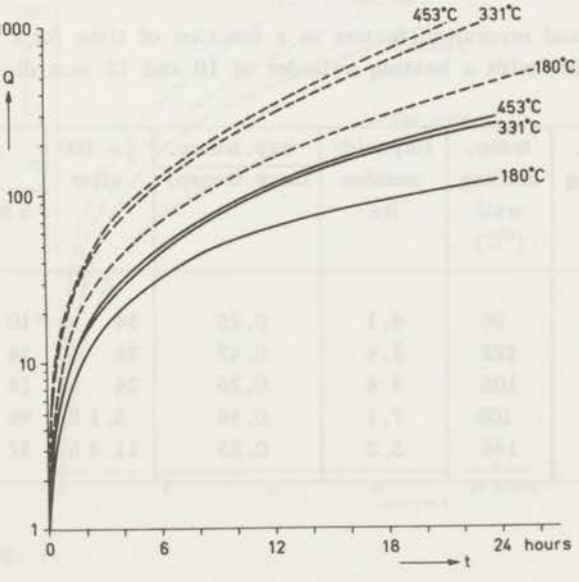

Fig. 5

Separation as a function of time for a column with H' = 66.68 g and r_h = 7.0 mm. – – – – – theory ———— experiment.

C. Column at higher overall temperature

To reduce the effects of adsorbing and desorbing CO_2 molecules on the cold wall of the column experiments have been done at a higher overall temperature. Instead of water in the cooling circuit between the outer walls of the column oil was used. It was kept at a constant temperature, which could be set at between 90° and 150 °C by means of a thermostat.

The experiments were carried out with a heating cylinder having a diameter of 12 mm and a lower volume of 121 cc. The results are plotted in Fig. 6 and are also tabulated in Table II.4.

Comparing these experiments with those of Section 2 A one finds that the Reynolds numbers are between 3.4 and 4.1, whereas the initial transport is a factor four lower - in Eq. (1.18) $\overline{T}$ is increased and m is reduced. These two phenomena influence the result more than the increase in optimum pressure so that the separations are a factor three to four worse than those with normal cooling water. As it was found that the Reynolds number was the dominating factor, better results could be expected with a wider gap d. The experiments were repeated with a heating cylinder of 10 mm diameter. In Table II.4 it can be seen that the enrichments are much better than in the 12 mm column, although Fig. 7 shows that the separation is less than expected theoretically.

TABLE II.4

Initial transport and separation factors as a function of time for a column at a higher overall temperature with a heating cylinder of 10 and 12 mm diameter.

diameter heating rod (mm)	temp. heating rod (°C)	temp. cooling wall (°C)	Reynolds number Re	exp. transp. / theor. transp.	q = 100 after	separation after		
						5 hrs	10 hrs	15 hrs
12	294	96	4.1	0.29	34 h.	10.3	19	28
"	403	122	3.4	0.47	28 h.	14	26	42
"	528	105	3.4	0.26	24 h.	18	37	59
10	456	105	7.1	0.36	5.1 h.	98	235	405
"	493	146	5.2	0.23	11.3 h.	37	86	143

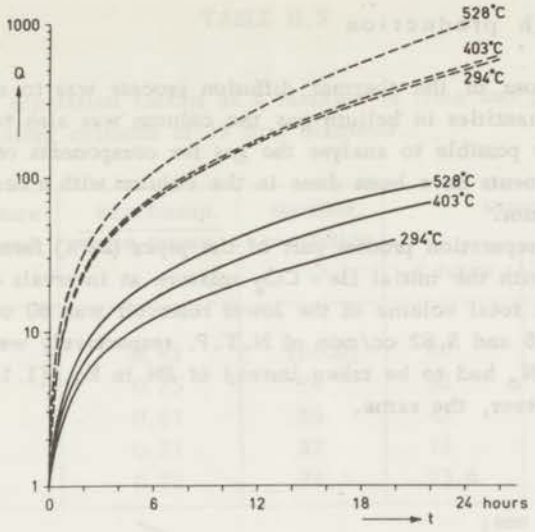

Fig. 6

Separation as a function of time for a column at higher overall temperature with $r_h = 6.0$ mm.
theory _ _ _ _ _ _ _ experiment. _____

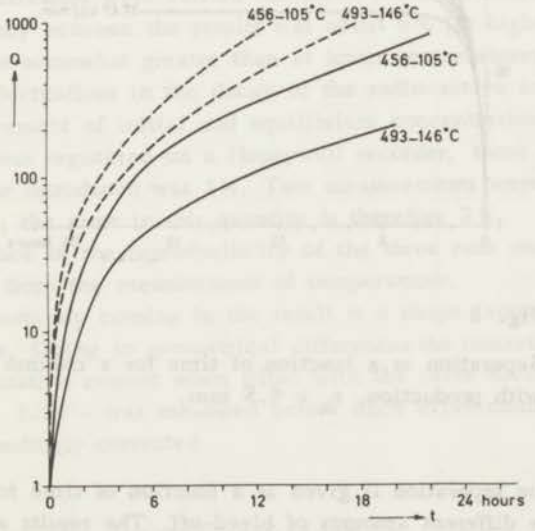

Fig. 7

Separation as a function of time for a column at higher overall temperature with $r_h = 5.0$ mm.
theory _ _ _ _ _ _ experiment. _____

D. Column with production

As the purpose of the thermal diffusion process was to extend the range of measuring trace quantities in helium gas the column was also tested for bleed-off so that it would be possible to analyse the gas for components other than CO_2.

The experiments have been done in the column with a heating cylinder having a diameter of 13 mm.

During the separation process part of the pipes (22 %) forming the lower reservoir were flushed with the initial He - CO_2 mixture at intervals of 20, 30, 45 and 60 minutes. As the total volume of the lower reservoir was 80 cc this meant that 17.47, 11.64, 7.76 and 5.82 cc/min of N.T.P. respectively were blown off, bearing in mind that PN_o had to be taken instead of PN in Eq. (1.19). The result for Eq. (1.21) is, however, the same.

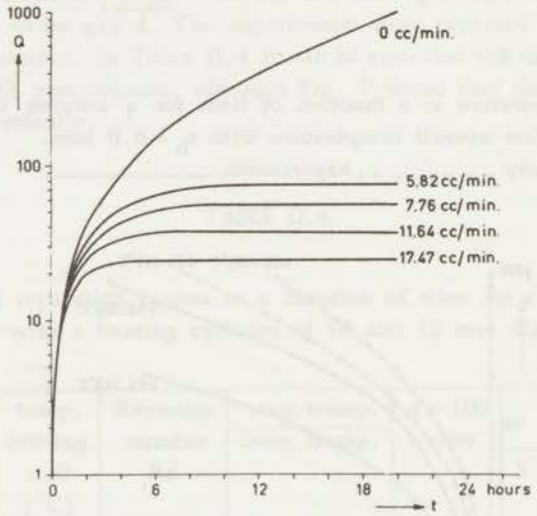

Fig. 8

Separation as a function of time for a column with production, r_h = 6.5 mm.

In Fig. 8 the separation is given as a function of time for the column at total reflux and the different amounts of bleed-off. The results are summarized in Table II.5

TABLE II.5

Initial transport and separation factors as a function of time and production rate for a column with a heating cylinder of 13 mm diameter.

bleed-off (cc/min)	temperature heating rod (°C)	exp. transp. / theor. transp.	equilibr. separation Q	separation after		
				4 hours	8 hours	12 hours
0	266	0.83	(6600)	86	220	405
5.82	267	0.75	74	52	70	74
7.76	266	0.63	55	42	55	55
11.64	266	0.71	37	33	37	37
17.47	263	0.72	24.5	23.6	24.5	24.5

3. DISCUSSION OF THE EXPERIMENTS

A. Discussion of errors and uncertainties

All the experiments were carried out three times (or more) at one temperature. The discrepancy between the results was about 6 % (at higher temperatures of the heating cylinder somewhat greater than at lower temperatures).

Statistical fluctuations in the decay of the radio-active carbon led to variations in the measurement of initial and equilibrium concentration of CO_2, but as the whole process was registered on a Honeywell recorder, these variations could be averaged. The error introduced was 1 %. Two measurements were involved in the determination of Q; the error in this quantity is therefore 2 %.

The difference in the reproducibility of the three runs must be due to the uncertainty arising from the measurement of temperatures.

A third uncertainty coming in the result is a shape factor between the two ionization chambers. Owing to geometrical differences the ionization chambers did not show the same ionization current when filled with the same helium - $^{14}CO_2$ mixture. The shape factor - 1.24 - was measured before each experiment and the separation factor was correspondingly corrected.

B. Discussion of the initial transport

In Table I.2 the difference is given for c_1 calculated according to formulas by three different writers. The initial transport for Jones and Furry is larger than for the other authors. The experimental values in Tables II.2, 3, 4, 5 are compared

with the theory of Fleischmann and Jensen. The ratio between experiment and theory is 70 %, except for the column at a higher overall temperature. With Jones and Furry's theory the observed efficiency is only 55 % and with Slieker's 67 %. Although the authors made different approximations in their formulas for c_1, the agreement with experiment is bad. Better results can only be expected when an exact derivation for the initial transport in concentric cylinder columns is available.

C. Discussion of the equilibrium separation factor and the relaxation time

Although c_1 according to Jones and Furry is greater than according to the other authors the equilibrium separation factor $\ln Q = (c_1/c_5)Z$ is smaller. This is due to c_3, which is the dominating factor in c_5. In Table II.6 ln Q is given calculated by Jones' and Fleischmann's theory and taken from experiment.

The agreement between theory and experiment is poor; only the column with a heating rod of 13 mm diameter produced good results. Hence it is shown that an imperfection in the construction of the thermal diffusion column influences the initial transport less than the stationary state separation.

TABLE II.6

ln Q experimental and theoretical, according to the theories of Jones and Furry, and of Fleischmann.

experiment	temperature heating rod (°C)	diameter heating rod (mm)	ln Q (exp)	ln Q (theor) Jones & Furry	ln Q (theor) Fleischmann
Sec. 2.B	157	13	8.5	9.58	10.80
	280	"	10.6	16.00	18.80
	298	"	11.0	17.11	20.01
	180	14	>6.1	18.46	21.75
	331	"	6.8	35.85	39.52
	453	"	>7.4	52.06	57.52
Sec. 2.C	294	12	3.7	13.80	16.25
	403	"	4:2	17.41	22.88
	528	"	4.7	26.97	32.05
	456	10	6.9	9.48	10.47
	493	"	5.7	10.99	14.86

Dickel [33) 34)] treats a theory of the asymmetric separation column. By supposing that parasitic currents result from irregularities in the distance between hot and cold walls and from local slight temperature differences in the latter, he shows that the initial transport is practically unaffected, while the separation factor is considerably diminished. This theory seems to be confirmed by our experiments.

The relaxation time was calculated with Eq. (2.3), because Q is very large for most of the experiments. Eq. (2.3) states that the time taken to achieve a separation q is inversely proportional to c_1. For our experiments the discrepancy between empirical and theoretical relaxation time would be even larger by Jones and Furry's formulas.

TABLE II.7

Introduction of a $H_{eff.}$ in Eq. (1.26) and (1.29) so that theory and experiment coincide.

experiment	$2\,r_h$ (mm)	T_2 (°C)	$\frac{H_{eff.}}{H}$	length of column involved
Sec. 2.A	13	158	0.9209	0 cm
	"	273	0.8315	0 "
	"	419	0.6286	0 "
	12	177	1.6609	70.6 "
	"	265	1.2837	16.2 "
	"	303	0.9025	0 "
Sec. 2.B	13	157	0.7708	0 "
	"	280	0.9089	0 "
	"	298	1.0634	5.9 "
	14	180	1.9130	81.7 "
	"	331	1.0638	6.9 "
	"	453	1.0765	9.4 "
Sec. 2.C	12	294	1.2906	27.9 "
	"	403	2.0128	111.4 "
	"	528	1.1154	14.0 "
	10	456	0.5477	0 "
	"	493	0.5616	0 "

The calculations of the length of time taken to reach the steady state involves the assumption of the quasi-stationary state in the column, which means that the

transport is assumed to be independent of z, $\tau \neq f(z)$. This condition is fulfilled when $H > c_6 Z$ or when $\frac{2 HH'}{H + H'} > c_6 Z$, according to Jones and Furry [22] (p. 181).

A second method, however, gives the relaxation time without using the quasi-stationary state assumption, treating the general case of a square cascade, according to Cohen [24]. The formula is given as an infinite series, but too many terms have to be taken in the case of large Q's. Only when $H' = \infty$ can a result be given, which closely resembles Jones and Furry's equation (1.26) with a relaxation time t_r also depending on the hold-up in the column.

A $H_{eff.}$ is therefore now introduced because in the experiments described in this chapter H and $c_6 Z$ are of the same order. Eq. (1.26) and (1.29) have been used, where t is taken from the experiments for q = 100 or 50. The results are shown in Table II.7.

For 8 of the 17 experiments $H_{eff.} < H$, for the others $H_{eff.} > H$, which means that part of the column must be considered as lower reservoir so that experimental and theoretical relaxation time coincide. No explanation can be found as to why $H_{eff.}/H$ is not constant.

D. Discussion of the column with production

Equation (1.21) gives the relation between the production rate P and the separation Q. From Table II.5 the following experimental results are taken: bleed-off or production rate P and the transport factor c_1 in order to calculate the normalized production rate $\psi = P/c_1$. With Eq. (1.21) Q has been calculated as a function of ψ, using $6600 \approx e^{8.80}$ for $e^{2\epsilon Z}$. The result is given in Table II.8, where it is compared with the experimental separation Q_{exp}. It can be seen that agreement between theory and experiment is quite good.

TABLE II.8

Theoretical and experimental separation factors as a function of the production rate for a column with r_h = 6.5 mm at 266 °C.

bleed-off (cc/min)	production (g/hour)	c_1 (g/hour)	$\psi = P/c_1$	Q_{theor}	Q_{exp}
5.82	0.058	5.30	0.011	91	74
7.76	0.077	4.46	0.017	59	55
11.64	0.116	5.00	0.023	44	37
17.47	0.174	5.00	0.035	29	24.5

For large equilibrium separations the term unity in the denominator of Eq. (1.21) can be omitted so that it can be written as $Q = (1 + \psi)/\psi$. For small production rates ψ, Q is inversely proportional to ψ. The experiments obey this law.

Finally the separation without production can be compared with the column described in Sec. 2.B where the lower volume is 114 cc. From Fig. 8 it follows that Q = 100 was reached after 4.5 hours, when H = 80 cc. The ratio between relaxation time (4.5 or 6.5 hours) and lower reservoir (80 cc or 114 cc) for both columns is the same to within 1.5 %.

CHAPTER III

THEORY OF THE THERMAL DIFFUSION FACTOR

1. THE THERMAL DIFFUSION FACTOR AT LOW DENSITIES

The theory of the thermal diffusion factor α introduced in chapter I is quite complicated. Different approximations have been made, sometimes adapted to the mixtures with which the experiments have been carried out.

The most elementary theory, considering the molecules as elastic spheres of the same diameter, leads to

$$\alpha = 0.89 \frac{M_2 - M_1}{M_2 + M_1} \tag{3.1}$$

where M_1 and M_2 are the molar masses of the components. It means that α is independent of the temperature, the concentration and the pressure.

The most well-known expression for α comes from the first approximation of the solution of the Boltzmann equation. It is found under the following assumptions:

1. the density of the gas is so low that the effect of collisions involving more than two molecules is negligible;
2. the temperature is such that quantum effects do not need to be considered;
3. only certain types of distribution functions $f^{(N)}$ are considered by the assumption of "molecular chaos";
4. the molecules have no internal degrees of freedom, they have a spherical symmetry;
5. the intermolecular forces are only short-range;
6. the difference in position between two colliding molecules is not taken into account;
7. the flux vectors $\vec{\psi}_j$ contain only the first spatial derivatives of temperature, mass velocity and concentration.

The general expression for the first approximation of α can be found in the book of Chapman and Cowling [17] for example. Unlike Eq. (3.1) this expression for α is dependent on temperature and concentration. The intermolecular potential comes into the equation through the collision integrals $\Omega^{(l,r)}_{i,j}$. They are integrals of the differential cross section for a collision, weighted with a factor $1 - \cos^{l}\chi$ and averaged over the kinetic energy of the relative motion of the molecules. The lower indices refer to the type of molecules i and j, the index r to the power of the initial relative speed. The angle by which the molecules are deflected, χ, depends on the law of interaction between the particles.

The intermolecular potential model used in this thesis is the Lennard - Jones (6-12) potential:

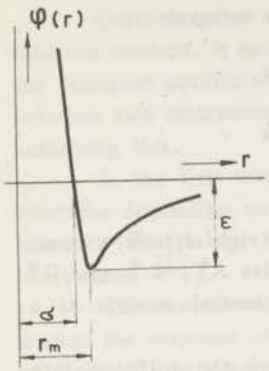

Fig. 9

The Lennard - Jones (12-6) potential model.

$$\phi(r) = 4\,\varepsilon \left\{ (\sigma/r)^{12} - (\sigma/r)^{6} \right\} \qquad (3.2)$$

where $\phi(r)$ is the potential energy of interaction between two particles at a distance r. The force constants are ε (the maximum energy of attraction at a distance $r = r_m$) and σ (the distance in Å where $\phi(r) = 0$) (Fig. 9). To get the potential between different kinds of molecules ε_{12} and σ_{12} have to be taken in Eq. (3.2) instead of ε and σ with

$$\sigma_{12} = \tfrac{1}{2}(\sigma_1 + \sigma_2) \qquad \varepsilon_{12} = \sqrt{\varepsilon_1 \cdot \varepsilon_2}\,. \qquad (3.3)$$

The thermal diffusion factor of dilute gases can be calculated following the procedure developed by Kihara [36], who got a simpler expression for the first approximation to α than the formula of Chapman and Cowling. For binary mixtures Kihara found:

$$\alpha = \frac{(6C^* - 5)\left\{ S_1 x_1 - S_2 x_2 \right\}}{Q_1 x_1^2 + Q_2 x_2^2 + Q_{12} x_1 x_2} \qquad (3.4)$$

in which

$$S_1 = \frac{M_1}{M_2}\sqrt{\frac{2M_2}{M_1 + M_2}}\left(\frac{\Omega^{(2,2)*}_{1,1}}{\Omega^{(1,1)*}_{1,2}}\right)\left(\frac{\sigma_1}{\sigma_{12}}\right)^2 - \frac{4M_1 M_2 A^*}{(M_1 + M_2)^2} - \frac{15M_2(M_2 - M_1)}{2(M_1 + M_2)^2}$$

$$Q_1 = \frac{2}{M_2(M_1 + M_2)}\sqrt{\frac{2M_2}{M_1 + M_2}}\left(\frac{\Omega^{(2,2)*}_{1,1}}{\Omega^{(1,1)*}_{1,2}}\right)\left(\frac{\sigma_1}{\sigma_{12}}\right)^2 (3M_2^2 + M_1^2 + \tfrac{8}{5}M_1 M_2 A^*)$$

$$Q_{12} = \frac{15(M_1 - M_2)^2}{(M_1 + M_2)^2} + \frac{32M_1 M_2 A^*}{(M_1 + M_2)^2} + \frac{8(M_1 + M_2)}{5\sqrt{M_1 M_2}}\,\frac{\Omega^{(2,2)*}_{1,1}\,\Omega^{(2,2)*}_{2,2}}{(\Omega^{(1,1)*}_{1,2})^2}\,\frac{\sigma_1^2\,\sigma_2^2}{\sigma_{12}^4}$$

$x_{1,2}$ = the mole fraction of component 1, 2.
S_2 and Q_2 are the same as S_1 and Q_1 after interchanging the subscripts which refer

to molecules 1 and 2. A^* and C^* are the ratios of collision integrals

$$A^* = \frac{\Omega^{(2,2)*}_{1,2}}{\Omega^{(1,1)*}_{1,2}} \qquad C^* = \frac{\Omega^{(1,2)*}_{1,2}}{\Omega^{(1,1)*}_{1,2}} \quad .$$

The superscript $*$ means that the values are divided by their rigid-sphere values.

The dependence of α on temperature is in the quantities A^*, C^* and Ω^*. They are tabulated in Hirschfelder's book [18] for different potential models as a function of $T^* = kT/\varepsilon$ (k is Boltzmann's constant).

α depends parametrically on the potential model through the collision integrals, it is clear that α is also influenced by the concentration, the size and the mass of the molecules.

There seems to be no dependence of α on the pressure. Experiments have shown that the thermal diffusion factor is pressure independent under atmospheric pressures and slightly above (Lugg [37]; Ibbs, Grew and Hirst [38]; Grew [39]; Drickamer and Hofto [12a]).

2. THE THERMAL DIFFUSION FACTOR AT MODERATELY HIGH PRESSURES

The theory of the transport properties at higher densities is a subject of intense study nowadays. In the last section the thermal diffusion factor has been derived from the Boltzmann equation, assuming that the mean free path of the molecules is large compared with its diameter, so that only binary collisions occur. To derive equations for the transport coefficients of a moderately dense gas ($p > 1$ atm) the Boltzmann equation has to be generalized with terms that include the effect of triple and higher order collisions. This can be done by the distribution function method.

Bogoliubov [40] starting from the Liouville equation, which he expanded in powers of the density, found a kinetic equation for the first distribution function that in lowest order of the density resulted in the Boltzmann equation. The theory has been commented and outlined again by Choh and Uhlenbeck [41].

A second method to derive the generalized Boltzmann equation has been given by Green [42] and Cohen [43], who use cluster expansions for the non-equilibrium distribution functions. Cohen has given the connection between Bogoliubov's and Green's method.

To calculate the transport coefficients the generalized Boltzmann equation can be solved by a solution according to Hilbert - Enskog [41]. The distribution function is then only dependent on the density $n(\vec{r};t)$, the average velocity $\vec{u}(\vec{r};t)$ and the temperature $T(\vec{r};t)$. In this way a set of hydrodynamic equations has been derived in which the transport coefficients appear as an expansion in the local density n. Explicit expressions, however, are only given for η and λ to general order in the density [44].

Quite another way of obtaining transport coefficients is the time correlation function method. It assumes that the system is initially in local equilibrium and gives the transport coefficients as very general expressions in terms of correlation functions between two microscopic quantities at different times. There are two methods for achieving this.

In the first way one starts with the Liouville equation and looks for special solutions depending on time only through the quantities $n(\vec{r};t)$, $\vec{u}(\vec{r};t)$ and $\varepsilon(\vec{r};t)$, where $\varepsilon(\vec{r};t)$ is the local energy density (Mori [45], Kirkwood [46], H.S. Green [47], Mc Lennan [48]).

The second way is the linear response theory according to Kubo [49], who studies the response of the system that is perturbed by some disturbance (mechanical or thermal). In the case of the mechanical disturbance (like an electrical field) the Kubo formalism is complete. However, the case of thermal disturbances is more complicated, owing to the statistical nature of the temperature itself.

Several investigators have shown that the correlation function method reduces to the well-known expressions at low density [45] [47] [50], but explicit expressions for the thermal diffusion factor have not yet been given. It is clear too nowadays that the distribution function method and the correlation function method lead to identical expressions [50], [51], [52], [53]. Both methods are worked out for dense binary gas mixtures [54].

An explicit expression for α has been given by Enskog [16], [17] and Thorne, who developed a theory of dense gases in which only binary collisions were considered. Enskog introduces corrections for the fact that the transfer of energy and momentum not only occurs between the collisions, but also during the collisions of the molecules. This "collisional transfer" mechanism is restricted to rigid spheres and multibody collisions have not been considered.

Two corrections can be made to the Boltzmann equation:

1. at the moment of collision the centres of the two molecules are not at the same point. When the first molecule is at $\vec{r}$, the centre of the second molecule is at $\vec{r} - \sigma\vec{k}$, where the unit vector is denoted by $\vec{k}$ and the diameter of the molecules by . The distribution function $f(\vec{c}_1, \vec{r})$ has to be replaced by $f(\vec{c}_1, \vec{r} - \sigma\vec{k})$;
2. in a dense gas the volume in which any one molecule can be, is reduced by the total volume of the other molecules. This effect increases the probability of a collision. The frequency of collisions is increased by a factor Y, which is evaluated at the point $\vec{r} - \frac{1}{2}\sigma\vec{k}$ at which the molecules collide. Y is a function of the number density $n(\vec{r}, t)$ and of σ.

The Boltzmann equation thus obtained can be solved in first approximation by expanding the distribution function $f(\vec{c}, \vec{r}, t) = f^{(o)}(\vec{c})\ [1 + \Phi(\vec{c}, \vec{r}, t)]$ leading to expressions for the viscosity and the thermal conductivity of dense pure gases.

H.H. Thorne generalizes Enskog's theory to mixtures for diffusion, thermal diffusion, thermal conductivity and viscosity. The first approximation to α is given by:

$$\alpha = \frac{(6C^* - 5)\left\{ S_1' x_1 - S_2' x_2 \right\}}{Y_1 Q_1 x_1^2 + Y_2 Q_2 x_2^2 + (Y_{12} Q_{12}' + Y_1 Y_2 / Y_{12} Q_{12}'') x_1 x_2} \qquad (3.5)$$

in which

$$S_1' = \frac{Y_1 Z_2}{Y_{12}} \frac{M_1}{M_2} \sqrt{\frac{2 M_2}{M_1 + M_2}} \left(\frac{\Omega_{1,1}^{(2,2)^*}}{\Omega_{1,2}^{(1,1)^*}} \right) \left(\frac{\sigma_1}{\sigma_{12}} \right)^2 - \frac{4 Z_1 M_1 M_2 A^*}{(M_1 + M_2)^2} -$$

$$- \frac{15 Z_1 M_2 (M_2 - M_1)}{2 (M_1 + M_2)^2}$$

$$Q_1 = \frac{2}{M_2 (M_1 + M_2)} \sqrt{\frac{2 M_2}{M_1 + M_2}} \left(\frac{\Omega_{1,1}^{(2,2)^*}}{\Omega_{1,2}^{(1,1)^*}} \right) \left(\frac{\sigma_1}{\sigma_{12}} \right)^2 \times$$

$$\times \left[3 M_2^2 + (2.5 - 1.2 B^*) M_1^2 + \frac{8}{5} M_1 M_2 A^* \right]$$

$$Q_{12}' = \frac{1}{(M_1 + M_2)^2} \left[15 (M_1 - M_2)^2 (2.5 - 1.2 B^*) + \right.$$

$$\left. + 32 M_1 M_2 (1.375 - 0.3 B^*) A^* \right]$$

$$Q_{12}'' = \frac{8 (M_1 + M_2)}{5 \sqrt{M_1 M_2}} \frac{\Omega_{1,1}^{(2,2)^*} \Omega_{2,2}^{(2,2)^*}}{\left(\Omega_{1,2}^{(1,1)^*} \right)^2} \frac{\sigma_1^2 \sigma_2^2}{\sigma_{12}^4}$$

$$Y_1 = 1 + \frac{5}{12} \pi n_1 \sigma_1^3 + \frac{\pi}{12} n_2 (\sigma_1^3 + 16 \sigma_{12}^3 - 12 \sigma_{12}^2 \sigma_1) + \ldots\ldots$$

$$Y_{12} = 1 + \frac{\pi}{12} n_1 \sigma_1^3 (8 - 3 \sigma_1 / \sigma_{12}) + \frac{\pi}{12} n_2 \sigma_2^3 (8 - 3 \sigma_2 / \sigma_{12}) + \ldots\ldots$$

$$Z_1 = 1 + \frac{2}{5}\pi\, n_1\, \sigma_1^3\, Y_1 + \frac{8}{5}\pi\, n_2\, \sigma_{12}^3\, \frac{M_1 M_2}{(M_1 + M_2)^2}\, Y_{12}$$

The relations for S_2', Q_2, Y_2 and Z_2 are obtained from those for S_1', Q_1, Y_1 and Z_1 by an interchange of the subscripts which refer to molecules 1 and 2.

$$B^* = \frac{5\,\Omega_{1,2}^{(1,2)^*} - 4\,\Omega_{1,2}^{(1,3)^*}}{\Omega_{1,2}^{(1,1)^*}}$$

n_i is the number density of the molecules, which is the number of molecules in the unit of volume.

The equation is of the same form as Eq. (3.4), but with a pressure dependence of α coming in the formula through Y_i and Z_i. At one atmosphere Y_i and Z_i differ only 0.15% from unity. When one puts $Y_i = Z_i = 1$ in Eq. (3.5) it becomes nearly equal to Eq. (3.4). The only difference is the factor $2.5 - 1.2\,B^*$. In the Kihara approximation this is taken unity by giving B^* its maxwellian model value of 5/4.

3. PHENOMENOLOGICAL EQUATIONS FOR α

A. Non-equilibrium thermodynamics

The thermodynamics of irreversible processes predicts only the relationships that exist among the transport coefficients. Therefore, the result contains phenomenological coefficients which cannot be evaluated theoretically.

Consider a diffusion process in a binary gas mixture with no external forces. According to the monograph of De Groot [56], following his notation, the fluxes of matter and heat are given by the phenomenological equations.

$$\vec{J}_i = \sum_{k=1}^{2} L_{ik}\, \vec{X}_k + L_{iu}\, \vec{X}_u \qquad (i = 1,2)$$

$$\vec{J}_q = \sum_{k=1}^{2} L_{uk}\, \vec{X}_k + L_{uu}\, \vec{X}_u \qquad (3.6)$$

L_{ik} are coefficients for which the Onsager relations $L_{ik} = L_{ki}$ and $L_{iu} = L_{ui}$ are valid. $\vec{X}_k$, $\vec{X}_u$ are the thermodynamic forces or affinities.

$$\vec{X}_k = - T \text{ grad } \frac{\mu_k}{T}$$
$$\vec{X}_u = - \frac{1}{T} \text{ grad } T \qquad (3.7)$$

μ_k is the chemical potential of component k per unit mass.

The fluxes are defined with respect to the centre of mass velocity $\vec{v}$, which follows from

$$\rho \vec{v} = \rho_1 \vec{v}_1 + \rho_2 \vec{v}_2 \quad ,$$

where ρ is the total density of the mixture
ρ_k the density of component k
$\vec{v}_k$ the velocity of component k.

Consequently:

$$\sum_{k=1}^{2} L_{ik} = 0 \qquad (i = 1, 2, u)$$

and $\vec{J}_1 = - \vec{J}_2$.

Introducing the new quantity $q_1^* = \frac{L_{1u}}{L_{11}}$ one can write the fluxes as

$$\vec{J}_1 = - \vec{J}_2 = L_{11} (\vec{X}_1 - \vec{X}_2 + q_1^* \vec{X}_u)$$
$$\vec{J}_q = q_1^* \vec{J}_1 + (L_{uu} - L_{1u} q_1^*) \vec{X}_u \qquad (3.8)$$

The quantity q_1^*, which now appears in the equation for both the mass flux and the heat flux, is called the heat of transfer. It can be interpreted as the heat transported with the unity of mass of component 1 at uniform temperature.

The affinity $\vec{X}_k$ can be rewritten by the substitution of

$$\text{grad } \mu_k = - s_k \text{ grad } T + v_k \text{ grad } p + \left(\frac{\partial \mu_k}{\partial c_1}\right)_{T,p} \text{ grad } c_1 \qquad (3.9)$$

with s_k the partial specific entropy of k,
v_k the partial specific volume of component k,
c_1 the concentration of component 1 (mass fraction).

Assuming that the pressure is uniform and using Eq. (3.7) and (3.9) the following expression for the mass flux can be obtained:

$$\vec{J}_1 = - L_{11} \left\{ \frac{\partial(\mu_1 - \mu_2)}{\partial c_1} \operatorname{grad} c_1 + (q_1^* - h_1 + h_2) \frac{\operatorname{grad} T}{T} \right\} \tag{3.10}$$

where h_k is the partial specific enthalpy of component k.

For the heat flux two different conditions must be considered; the initial state when grad $c_1 = 0$ and the stationary state when $\vec{J}_1 = 0$.

$$\begin{aligned} (\vec{J}_q)_{\nabla c_1 = o} &= - \left(L_{uu} - L_{1u} (h_1 - h_2) \right) \frac{\operatorname{grad} T}{T} \\ (\vec{J}_q)_{\vec{J}_1 = o} &= - \left(L_{uu} - L_{1u} q_1^* \right) \frac{\operatorname{grad} T}{T} \end{aligned} \tag{3.11}$$

The diffusion coefficient D_{12} and the thermal diffusion coefficient D_T are defined by:

$$\begin{aligned} \rho D_{12} &= L_{11} \frac{\partial(\mu_1 - \mu_2)}{\partial c_1} \\ \frac{\rho D_T}{T} &= L_{11} \frac{q_1^* - h_1 + h_2}{T} \end{aligned} \tag{3.12}$$

so that the thermal diffusion factor α is:

$$\alpha = \frac{D_T}{D_{12} c_1 (1 - c_1)} = \frac{q_1^* - h_1 + h_2}{c_1 (1 - c_1) \dfrac{\partial(\mu_1 - \mu_2)}{\partial c_1}} = \frac{q_1^* - h_1 + h_2}{c_1 \dfrac{\partial \mu_1}{\partial c_1}} \tag{3.13}$$

When both components and the mixture can be considered as ideal gases the thermodynamical constants are:

$$h_1 = \text{const.} + \frac{5}{2} \frac{R T}{M_1} \qquad h_2 = \text{const.} + \frac{5}{2} \frac{R T}{M_2}$$

$$c_1 \frac{\partial \mu_1}{\partial c_1} = \frac{M}{M_1 M_2} x_1 \frac{\partial \tilde{\mu}_1}{\partial x_1} = \frac{M}{M_1 M_2} R T$$

where $M = M_1 x_1 + M_2 x_2$, the molar mass of the mixture, $\tilde{\mu}_1$ = chemical potential of component 1 per unit mole.

Now, the pressure dependence of α comes into the expression through h_i and μ_i. At high pressures the corrections on α can be given by taking for the thermodynamic quantities their values for real gases instead of ideal gases. The only difficult point in the formula is the quantity q_1^*, which cannot be evaluated numerically.

B. Equations involving further assumptions

Haase [15], Drickamer [9b] and Kotousov [55] have used Eq. (3.13) based on the theory of thermodynamics of irreversible processes to explain the pressure dependence of α. Therefore, they had to make some assumptions.

Haase [15] and Drickamer [9b] write for gases, which behave ideally in equilibrium:

$$\alpha_o = \frac{(q_1^{*o} - h_1^o + h_2^o) M_1 M_2}{M R T}$$

where the superscript o means the value at low densities. They assume that q_1^* is independent of the density of the system, so that one can put $q_1^* = q_1^{*o}$. Doing this it is possible to split the thermal diffusion factor α into an ideal part and a part depending on the deviations of the ideal gas laws. The result is:

$$\alpha = \frac{\alpha_o}{1 + x_1 x_2 \frac{\partial^2 \ln f}{\partial x_1^2}} + \frac{(h_2 - h_2^o) - (h_1 - h_1^o)}{c_1 \frac{\partial \mu_1}{\partial c_1}} \qquad (3.14)$$

where the thermodynamic relation [57]

$$x_1 \frac{\partial \tilde{\mu}_1}{\partial x_1} = R T \left[1 + x_1 x_2 \frac{\partial^2 \ln f}{\partial x_1^2} \right]$$

has been used, with f the fugacity of the mixture.

Kotousov [55] introduces the heat of transfer in Eq. (3.6) by substituting

$$L_{1u} = L_{11} Q_1^* + L_{12} Q_2^*$$

$$L_{2u} = L_{12} Q_1^* + L_{22} Q_2^*$$

In this way he finds for α

$$\alpha = \frac{M_1 Q_1^* - M_2 Q_2^* - M_1 h_1 + M_2 h_2}{x_1 \frac{\partial \tilde{\mu}_1}{\partial x_1}}$$

From the definition of the thermal conductivity coefficient λ in Eq. (3.11) he is able to express λ grad T also in terms of $M_1 Q_1^*$ and $M_2 Q_2^*$. He uses the relation

$$\frac{\text{grad } T}{\text{grad } x_1} = - \frac{\frac{\partial}{\partial x_1} (H_1 - H_2)}{\frac{\partial}{\partial T} (H_1 - H_2)}$$

and ignores the term $\frac{K_T \text{ grad } T}{T}$ in comparison with grad x_1. His result is:

$$\alpha = \frac{\frac{\partial}{\partial x_1} (H_1 - H_2)}{\frac{\partial}{\partial T} (H_1 - H_2)} \frac{\lambda}{\rho D_{12}} \frac{M}{x_1 \frac{\partial \tilde{\mu}_1}{\partial x_1}} \qquad (3.15)$$

where $H_i = M_i h_i$ is the partial molar enthalpy of component i.

C. Fugacity method

Becker [11] proves that a separation in a gas mixture in a temperature gradient occurs when one component obeys the ideal gas laws and the other component the Van der Waals equation of state

$$p = \frac{R T}{V - b} - \frac{a}{V^2} \quad .$$

As he assumes only collisions between molecules of the same kind, this separation cannot be due to thermal diffusion. The thermal diffusion separation is based on collisions between unlike molecules. In his derivation of the formulas he ignores, however, the co-volume b in the Van der Waals equation, the non-ideality of the second component and the interaction terms in a and b.

Becker's theory can be completed with the following imaginary experiment. Consider two vessels at different temperatures T_1 and T_2 ($T_2 > T_1$) with a non-ideal gas mixture. Let the transition from temperature T_2 to T_1 be via the hypothetically intermediate states where the gas is regarded as ideal (Fig. 10). Between T_2 real and ideal and between T_1 ideal and real there is no thermal diffusion. Between T_2 and T_1 in the ideal state there is a separation Q_{ideal} due to ordinary thermal diffusion. At T_1 and T_2 the laws of thermodynamics can be used. Together with the fact that the fugacity for an ideal gas is equal to the pressure, it is clear that the following relation should hold:

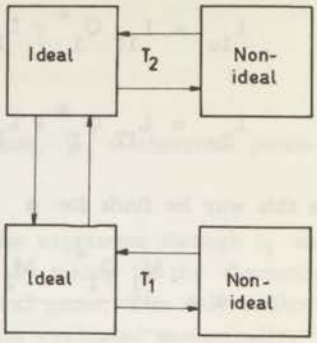

Fig. 10

Diagram to illustrate the calculation of the "equilibrium separation" of a real gas mixture in a temperature gradient.

$$\left[\left(\frac{f_1}{f_2}\right)_c\right]_{\text{non-ideal}} = \left[\left(\frac{f_1}{f_2}\right)_c\right]_{\text{ideal}} = \left[\left(\frac{f_1}{f_2}\right)_h\right]_{\text{ideal}} = \left[\left(\frac{f_1}{f_2}\right)_h\right]_{\text{non-ideal}} \qquad (3.16)$$

where $f_{1,2}$ = the fugacity of component 1,2 in the mixture and the subscripts c and h mean the values taken at T_1 and T_2.

As $$\ln f_i = \ln x_i + \ln p - \frac{1}{RT}\int_0^p \left(\frac{RT}{p} - V_i\right) dp$$

equation (3.16) states that

$$\ln\left(\frac{x_1}{x_2}\right)_h - \ln\left(\frac{x_1}{x_2}\right)_c = \ln Q_{real} =$$

$$= \frac{1}{RT_1}\int_0^p (V_1 - V_2)\, dp - \frac{1}{RT_2}\int_0^p (V_1 - V_2)\, dp \qquad (3.17)$$

with V_i the molar volume of component i.

Owing to the non-ideality of the gas there is a separation, which we call $\ln Q_{real}$. The ordinary thermal diffusion effect gives a separation $\ln Q_{ideal}$. When both separations are considered as additive the total separation is

$$\ln Q = \ln Q_{real} + \ln Q_{ideal} .$$

Consequently:

$$\alpha = \alpha_{real} + \alpha_{ideal} .$$

Introducing an equation of state in the general Eq. (3.17) one can calculate $\ln Q_{real}$.

Here the partial similarity between Haase's formula and the "fugacity" method must be pointed out. In the latter method grad $\ln f_1/f_2 = 0$ has been stated. As $\ln f_i = (\tilde{\mu}_i - \tilde{\mu}_i^{\circ})/RT$ condition (3.16) becomes

$$\operatorname{grad} \left(\frac{M_1 (\mu_1 - \mu_1^{\circ})}{T} - \frac{M_2 (\mu_2 - \mu_2^{\circ})}{T} \right) = 0 .$$

The substitution of (3.9) and the Gibbs- Duhem relation

$$c_1 \left(\frac{\partial \mu_1}{\partial c_1} \right)_{P,T} + c_2 \left(\frac{\partial \mu_2}{\partial c_1} \right)_{P,T} = 0$$

leads to (grad p = 0):

$$\frac{M_1 M_2}{M} c_1 \frac{\partial (\mu_1 - \mu_1^{\circ})}{\partial c_1} \frac{\operatorname{grad} c_1}{c_1 c_2} - \frac{M_1 (h_1 - h_1^{\circ}) - M_2 (h_2 - h_2^{\circ})}{T} \operatorname{grad} T = 0$$

or:

$$\alpha_{real} = \frac{\frac{M}{M_1} (h_2 - h_2^{\circ}) - \frac{M}{M_2} (h_1 - h_1^{\circ})}{c_1 \frac{\partial \mu_1}{\partial c_1}} \qquad (3.18)$$

There are two salient differences:
Haase's α_o and α_{real} are not additive since his α_o has been corrected by the factor $1 + x_1 x_2 \partial^2 \ln f / \partial x_1^2$, which becomes important at the highest pressures. The enthalpies in (3.18) are multiplied by the mass fraction M/M_i. This latter difference is largest at trace concentrations of one of the components.

D. Dimers

Drickamer [9a] has already stated that the clustering of molecules could influence the thermal diffusion process. Recently, Leckenby and Robbins [58] have observed double molecules (dimers) in the mass spectrum of CO_2 when the attractive Van der Waals interaction is important and the pressure high enough to produce a fraction of three-body collisions. Stogryn and Hirschfelder [59] and Kim et al. [60] have shown that a contribution to the density dependence of the viscosity in our pressure range can be caused by molecules colliding with a dimer (such as bound, metastable and orbiting pairs). The number density of dimers can be obtained from an equilibrium statistical mechanical calculation based on classical mechanics. When an equilibrium of the following form is assumed:

$$2\ CO_2 \rightleftarrows (CO_2)_2 \tag{3.19}$$

between two monomers and a dimer, this can contribute to an increase of α in three ways.

1. If all CO_2 molecules are dimers the thermal diffusion factor α can be calculated according to Eq. (3.4) with $M_2 = 88$ instead of 44. Due to the fact that the relative mass difference between He and CO_2 is already close to unity this effect leads only to an increase in α of 0.1.

2. When part of the CO_2 molecules are dimers the He - CO_2 mixture can be considered as a ternary mixture with particles having molar masses of 4, 44 and 88. The concentration of the dimer can be found from the equilibrium constant K^* for Eq. (3.19) as given by Kim and Ross. The effective thermal diffusion factors $\alpha_{ij}^{(tern.)}$ in a ternary mixture can be calculated, according to Van der Valk [61]. The simultaneous separations of monomers and dimers with respect to helium can be added, but the dimers have to be counted twice as they are analysed as two molecules of CO_2.

3. The dimer formation can be considered as a chemical reaction with an equilibrium constant $K_p = \dfrac{p\,(CO_2)_2}{(p\,CO_2)^2}$. The Van 't Hoff equation $\dfrac{d \ln K_p}{dT} = \dfrac{\Delta H}{RT^2}$ can be used to calculate the change in enthalpy or heat of reaction ΔH. Baranovski and De Vries [62] who have done experiments on Ar - NO_2 mixtures found that α increases very greatly as a consequence of the chemical reaction $2\ NO_2 \rightleftarrows N_2O_4$. They have derived a formula which gives a correction term α^1 to the thermal diffusion factor

$$\alpha^1 = -\frac{\Delta H}{RT} \frac{\alpha_d (1 - \alpha_d) \left[\dfrac{x_2}{x_1} (1 + \alpha_d) + 2 \right]}{4 \left(\dfrac{x_2}{x_1} + 1 \right)} \tag{3.20}$$

where α_d = degree of dissociation, that is the fraction of the total number of dimers $(CO_2)_2$ which are split up,

x_1 = mole fraction of the ideal (helium) component,

x_2 = mole fraction of the non-ideal component.

The difference in enthalpy between dimer and monomer $\Delta H/RT$ has been given in Stogryn's article [59] as a function of T^*. Kim and Ross give a reduced equilibrium constant

$$K^* = \frac{K_p V}{2/3\ \pi \sigma^3 N_A}$$

where V = the volume of one mole of the gas,

N_A = Avogadro's number.

With K^* it is possible to calculate the concentration of the dimer, from which α_d and α^1 follow.

CHAPTER IV

THE TWO-BULB APPARATUS; DESCRIPTION AND EXPERIMENTS

1. DESCRIPTION OF THE TWO-BULB APPARATUS

The two-bulb apparatus consists of two cylindrical stainless steel reservoirs connected by a tube and kept at temperatures T_1 and T_2 respectively ($T_2 > T_1$). To avoid convection the apparatus is mounted vertically with the hotter bulb at the top (see Fig. 11).

The lower reservoir V_1 is constructed as an ionization chamber to follow continuously the radioactive tracer concentration of the gas mixture. It has a coaxial collecting electrode, the distance between the electrodes being 3 mm. The wall of the chamber has a positive potential of 550 V with regard to the collector.

The upper reservoir V_2 is connected to an ionization chamber, I, to measure the radioactive tracer depletion. The ionization chambers together with the critical electrical components are maintained at room temperature for ease of operation. A water-cooling jacket W is therefore placed between the upper reservoir and the ionization chamber. The gas is flushed continuously through the ionization chamber by means of convective action through a by-pass B. The upper reservoir is placed in a specially built oven O filled with Vermiculite (asbestos) with one or two main heater windings H and one auxiliary winding (200 W). The oven is kept at a constant temperature with a contact thermometer T within 1 °C.

A water-cooled flange F is welded to the lower end of the connecting tube L. The cooling water is kept at a constant temperature T_3 ($T_1 < T_3 < T_2$) by a circulation thermostat.

Bulb V_1 is attached to the water-cooled flange via a Perspex (polymethyl methacrylate) flange P for the electric insulation. The apparatus is evacuated and filled through a side tube S entering the lower reservoir. The tube can be closed by needle valves.

Temperature readings are taken with the aid of a chromel-alumel thermocouple soldered to the hot bulb, and with an ordinary mercury thermometer for the lower reservoir, which is kept constantly at or slightly above room temperature. The pressure is measured with a Bourdon manometer.

The specifications of the two-bulb apparatus are:

hot reservoir V_2	: 51 cc
ionization chambers I	: 48 cc
lower reservoir V_1	: 83 cc
connecting tube L	: length 122 mm; diam. 11 mm
by-pass B	: length 61 cm; diam. 4 mm

Two different methods of analysis have been applied. The composition of the mixture with radioactive tracers was analysed with the ionization chambers. The con-

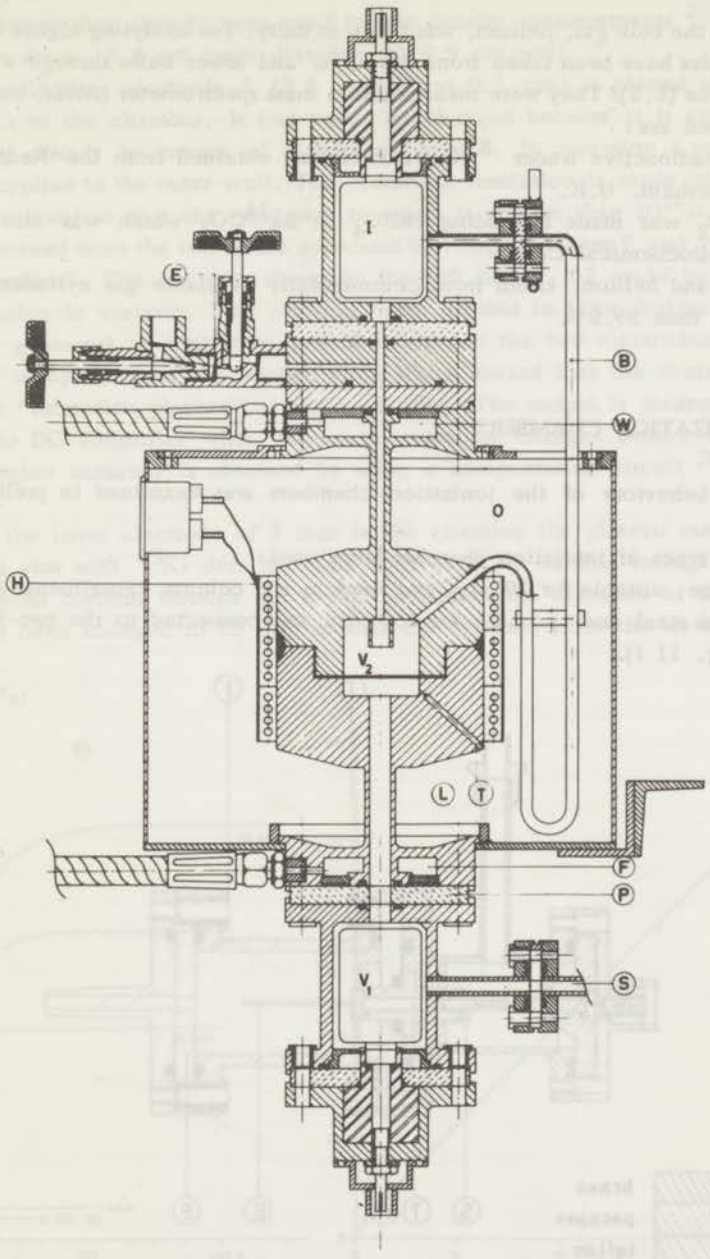

Fig. 11

The two-bulb apparatus.

B	by-pass	L	connecting tube	T	thermocouple
E	expansion-volume	O	oven	V_1	lower reservoir
F	water-cooled flange	P	Perspex flange	V_2	upper reservoir
H	heater	S	side tube	W	water-cooled flange
I	ionization chamber				

centration of the bulk gas, helium, was taken as unity. For analysing higher CO_2 concentrations samples have been taken from the upper and lower bulbs through a small expansion volume (E, S). They were measured in a mass spectrometer (Atlas, model CH_4). The gases used are:

The radioactive tracer ^{85}Kr, carrier-free obtained from the Radiochemical Centre, Amersham, U.K.

$^{14}CO_2$ was made by adding $HClO_4$ to $Ba^{14}CO_3$ which was also obtained from the Radiochemical Centre

CO_2 and helium, taken from commercially available gas cylinders; the purity was more than 99.9%.

2. THE IONIZATION CHAMBERS

The behaviour of the ionization chambers was examined in preliminary experiments.

Two types of ionization chamber were used:

1. a brass one, suitable for 20 atm and used in the column experiments (Fig. 12).
2. a stainless steel one, suitable for 150 atm and connected to the two-bulb apparatus (Fig. 11 I).

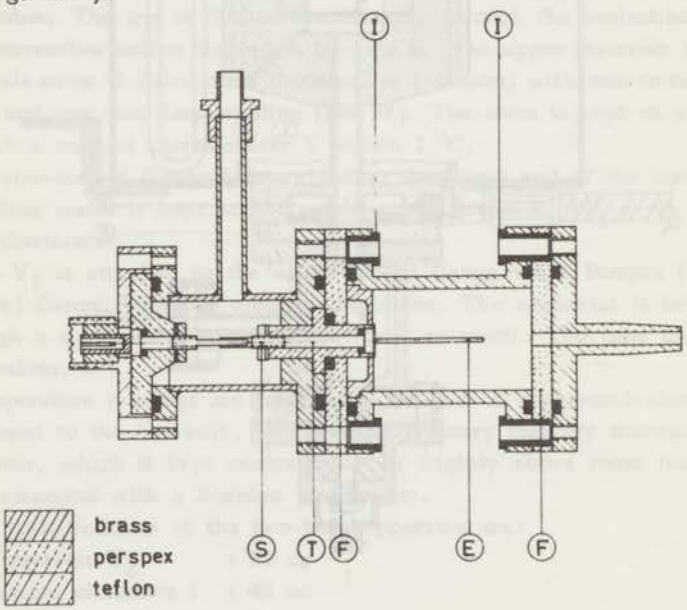

Fig. 12

The brass ionization chamber.

E collecting electrode
F Perspex flange
I insulating ferrule
S threaded joint
T Teflon insulation

The former has already been used in low density measurements [20) 63)]. It is cylindrical in shape, 3.2 cm inner diameter by 4.9 cm wall.

The collecting electrode E (3.4 cm, diam 0.3 cm) is placed so as to lie along the axis of the chamber. It can easily be changed because it is connected to the measuring circuit by means of a threaded joint S. In operation a positive high voltage V is applied to the outer wall. The electrical insulation is made of Teflon T (tetrafluoroethylene) so that the resistance to earth is greater than $10^{14}\,\Omega$. The high voltage is screened from the rest of the apparatus by Perspex flanges F and polyamide insulating ferrules I. The chamber shown on the left in Fig. 12 could be used for pre-amplification in vacuum. This part has been omitted in later designs. The radioactive tracer generates an ionization current I between the two electrodes. This current must be independent of the applied field which means that the chamber is operated at the "saturation plateau" of the I - V plot. The output is measured with a General Radio DC Amplifier when large concentration changes occur. For small separations higher accuracy is obtained by using a compensation circuit [20) 63)].

With the inner electrode of 3 mm in the chamber the plateau measured in helium at 20 atm with ^{85}Kr does not start until 1700 V. As this voltage causes too large background currents through the Teflon insulation the diameter of the inner electrode has been changed to 22 mm so that the distance from the wall was 5 mm on each side.

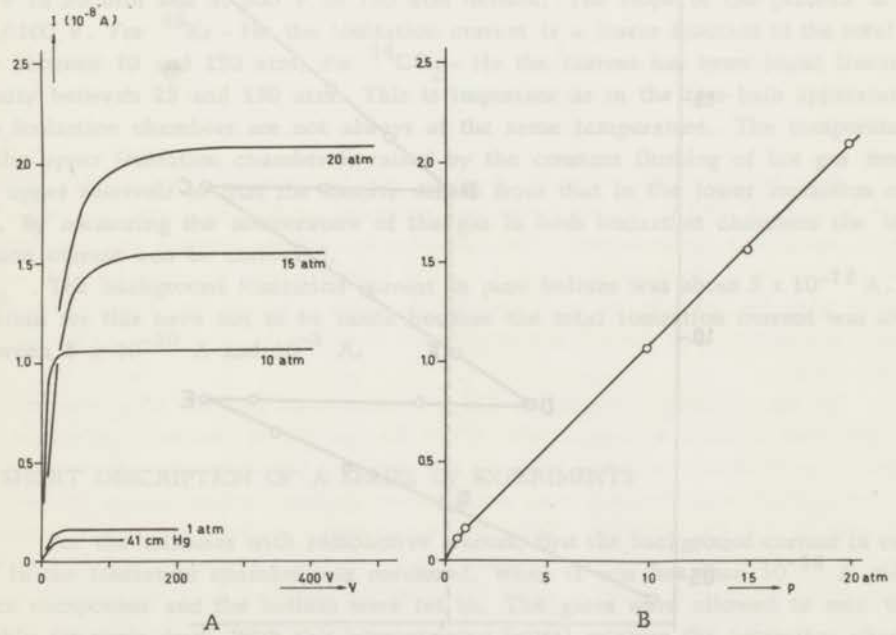

Fig. 13

A. Saturation curves of the brass ionization chamber. $^{14}CO_2$ in helium at various pressures

B. Pressure dependence of the ionization current at a constant ratio $^{14}CO_2$ - helium.

Measurements at different pressures with $^{14}CO_2$ showed that the plateau started at 30 V in 1 atm and at 340 V in 20 atm helium (Fig. 13 A). The ionization current plotted as a function of the pressure p (Fig. 13 B) produces a straight line between 0.5 and 20 atm, which means that I is proportional to the total density of the mixture.

Using the ionization chamber as an analysing instrument I should also be found to be proportional to the amount of radioactive tracer at a constant helium pressure. This can be tested by measuring the pressure dependence at a constant $^{14}CO_2$ - He ratio between 20 atm and 15 atm (A - B) (Fig. 14). At B pure helium is pressed into the ionization chamber up to 20 atm pressure (B - C), which means that the $^{14}CO_2$ - He ratio is then 75% of the initial ratio. The pressure dependence is measured again (C - D), after which pure helium is added (D - E) and so on. From the dilution of the $^{14}CO_2$ component the points F and G can be calculated and compared with experiment. The results given in Table IV.1 show that I is a linear function of the amount of radioactive tracer.

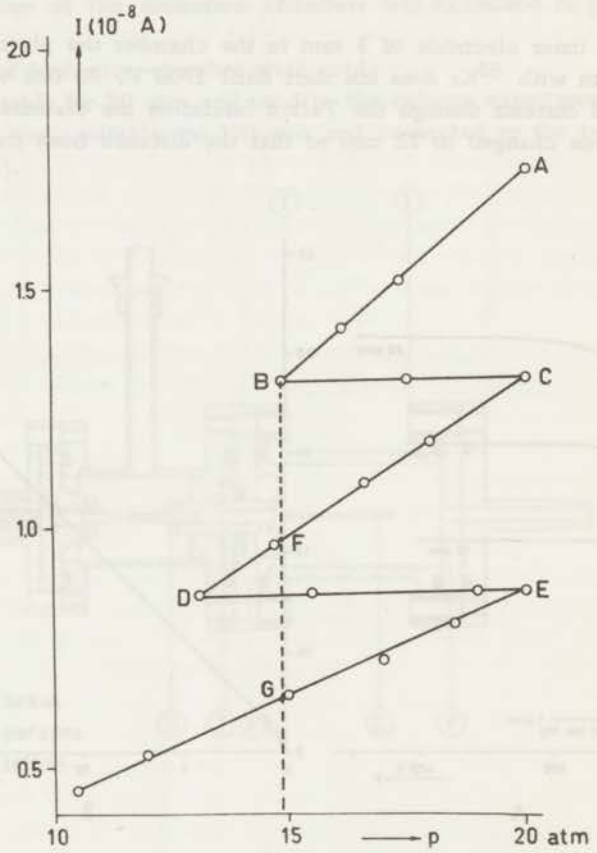

Fig. 14

Concentration dependence of the ionization current in $^{14}CO_2$ - helium at 14.9 atm. For description see text.

TABLE IV.1

Test on the linearity of ionization current.

point at 14.9 atm	ionization current	
	experimental	theoretical
B	1.31×10^{-8} A	-
F	0.980×10^{-8} A	0.971×10^{-8} A
G	0.645×10^{-8} A	0.636×10^{-8} A

As the brass ionization chamber could not be used for pressures up to 150 atm a stainless steel ionization chamber which differed only in size and minor details was designed. The outer wall is 7.0 cm long and has an internal diameter of 5.0 cm. The distance between the collecting electrode and the wall is 3 mm. The same calibrations were made up to 150 atm in this chamber. The saturation plateau begins at 90 V in 20 atm and at 550 V in 150 atm helium. The slope of the plateau is 2 % / 100 V. For ^{85}Kr - He the ionization current is a linear function of the total density between 10 and 150 atm, for $^{14}CO_2$ - He the current has been found linear with density between 25 and 150 atm. This is important as in the two-bulb apparatus the two ionization chambers are not always at the same temperature. The temperature of the upper ionization chamber is raised by the constant flushing of hot gas from the upper reservoir so that the density differs from that in the lower ionization chamber. By measuring the temperature of the gas in both ionization chambers the ionization current can be corrected.

The background ionization current in pure helium was about 5×10^{-12} A. Corrections for this have not to be made because the total ionization current was always between 5×10^{-10} A and 10^{-8} A.

3. SHORT DESCRIPTION OF A SERIES OF EXPERIMENTS

For the mixtures with radioactive tracers, first the background current in vacuum in the ionization chamber was measured. When it was less than 10^{-14} A the trace component and the helium were let in. The gases were allowed to mix thoroughly for some days. With this homogeneous initial mixture the ionization chamber factor was measured. Slight geometrical differences in the chambers led to different ionization currents. The ratio of these currents is called the ionization chamber factor. The experimental results (Fig. 15 and 16; Table IV.2 and IV.3) have been corrected for this. A series of experiments were carried out, starting with T_2 at 60 °C.

The relaxation time t_r of the experiment can be estimated from an equation given by Saxena and Mason [32].

$$t_r = \frac{L}{A}\left(\frac{T_1}{V_1} + \frac{T_2}{V_2}\right)^{-1} \left[\frac{T}{D_{12}}\right]_{av.}$$

where L is the length and A the cross-sectional area of the connecting tube,

$\left[\frac{T}{D_{12}}\right]_{av.}$ is the ratio of an average value of the temperature $T_1 < T < T_2$ and the binary diffusion coefficient in this temperature region.

For 150 atm, $T_1 = 303\ ^{o}K$ and $T_2 = 330\ ^{o}K$, $t_r = 40$ hours. t_r is the time taken to reach 1 - 1/e of the concentration difference of the stationary state. After 5 t_r the separation differs less than 1% from the stationary state separation. This time can be verified experimentally by measuring the ionization currents after regular intervals of time.

For trace components the separation factor Q reduces to

$$Q = \frac{\left[x_{CO_2}\right]_{T_1}}{\left[x_{CO_2}\right]_{T_2}} = \frac{I_1}{I_2} .$$

After reaching the stationary state T_2 was increased and the pressure lowered where necessary. The separation factor was measured in five to seven steps as a function of the higher temperature. The data of a run at one pressure and composition were plotted as a function of $\ln T_2 / T_1$. A smooth curve was constructed, where possible with the method of least squares, in order to cover the observed points as closely as possible. The thermal diffusion factor can then be evaluated as the tangent of the curve.

For the mixtures with higher CO_2 concentrations first the CO_2 was fed into the apparatus at uniform temperature. When the gas was in thermal equilibrium the pressure was read and helium added till the required concentration was reached. So the composition was obtained from two pressure readings, which meant that a relative error of 3% was possible. Then the temperature gradient was set and thermal diffusion allowed to reach its stationary state. In the stationary state the working pressure was read and samples were taken to be analysed in a mass spectrometer. The ratio of the peak lengths for mass 44 to that for mass 4 at T_1 divided by that ratio at T_2 is equal to Q.

4. EXPERIMENTAL RESULTS

A. Experiments with radioactive tracers

Experiments were carried out with helium - ^{85}Kr at pressures 42 atm and 135 atm. The ionization currents, measured in the initial mixture at the uniform room temperature of the entire apparatus, were different (see Section 3). At 42 atm $I_2 = 1.155\ I_1$, at 135 atm $I_2 = 1.121\ I_1$. Apparently the ionization chamber factor is slightly pressure dependent. This factor was taken into account in the experimental results which are given in Table IV.2 and illustrated in Fig. 15. Two straight lines can be drawn through the measured points; the tangent of the lines was calculated, producing:

α at 42 atm : 0.83 ± 0.01 $\quad 335 < T < 620\ ^{o}K$

α at 135 atm : 0.82 ± 0.02 $\quad 335 < T < 620\ ^{o}K$

Table IV.2 shows that the reproducibility in Q is 1%. The error in the thermal diffusion factor was calculated, assuming that the measured points were in a straight line. The uncertainty in α was found to be less than 2.5%.

TABLE IV.2

Experimental values of the separation factor for trace concentrations ^{85}Kr in helium at 42 atm and 135 atm.

42 atm $T_1 = 303\ ^{o}K$		135 atm $T_1 = 303\ ^{o}K$	
T_2 (^{o}K)	Q	T_2 (^{o}K)	Q
335	1.110	338	1.099
337	1.109	372	1.190
376	1.212	374	1.206
432	1.372	421	1.297
433	1.365	427	1.320
479	1.454	469	1.443
480	1.452	469	1.446
480	1.455	519	1.555
527	1.557	520	1.553
573	1.670	520	1.560
618	1.772	564	1.626
619	1.763	623	1.753

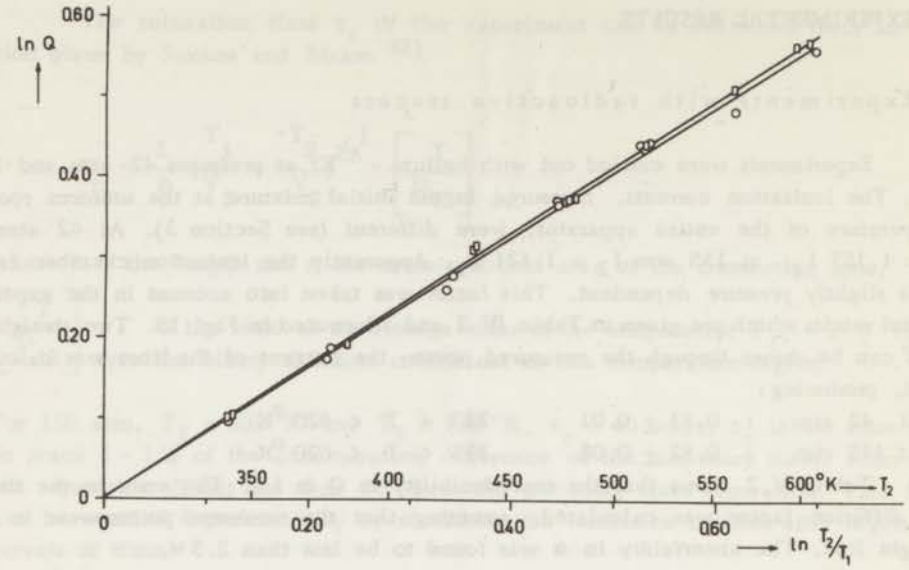

Fig. 15

Logarithm of the separation factor as a function of temperature for trace concentrations ^{85}Kr in helium. □ 42 atm ○ 135 atm.

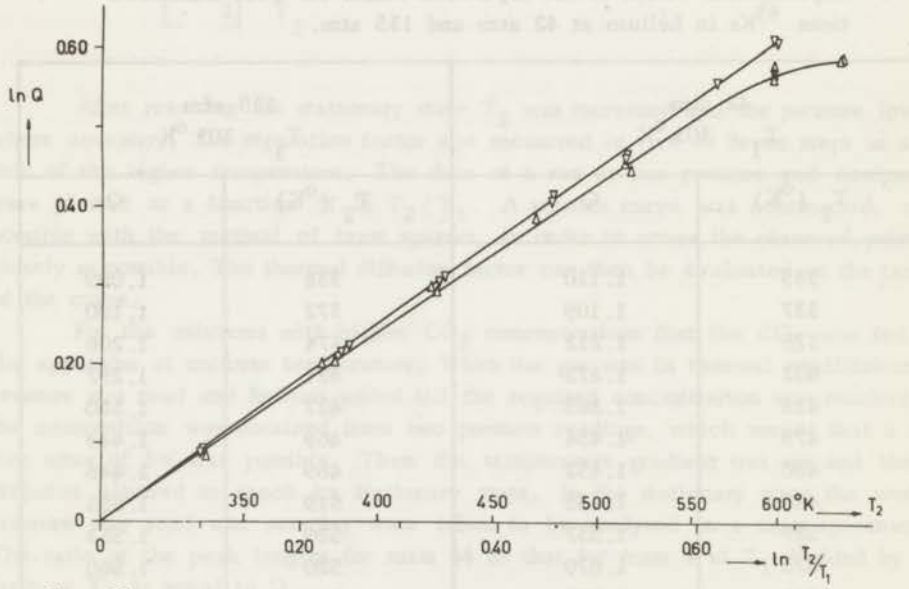

Fig. 16

Logarithm of the separation factor as a function of temperature for trace concentrations $^{14}CO_2$ in helium. ▽ 30 atm △ 134 atm.

For the mixture helium - $^{14}CO_2$ the thermal diffusion factor was measured at 30 atm and 134 atm. The ionization chamber factor was 1.154 at 30 atm and 1.112 at 134 atm; it decreased again with increasing pressure. The corrected values of Q are reported in Table IV.3 and shown in Fig. 16.

Fig. 16 shows that at 134 atm α is slightly temperature dependent. It occurs, however, at the limit of the high temperature range so that no certainty can be obtained.

For the temperature range, where α is constant, the tangents of the curves yield:

α at 30 atm : 0.916 ± 0.007 $\quad 330 < T < 620\ ^{o}K$

α at 134 atm : 0.88 ± 0.02 $\quad 330 < T < 520\ ^{o}K$

The reproducibility of the experiments is 1% as Table IV.3 shows. When it is assumed that all measured points at 30 atm and the measured points at 134 atm up to 525 ^{o}K are on a straight line the uncertainty in α is less than 2.5%.

TABLE IV.3

Experimental values of the separation factor for trace concentrations $^{14}CO_2$ in helium at 30 atm and 134 atm.

30 atm $T_1 = 305\ ^{o}K$		134 atm $T_1 = 301\ ^{o}K$	
T_2 (^{o}K)	Q	T_2 (^{o}K)	Q
330	1.095	330	1.086
330	1.097	381	1.222
382	1.246	381	1.226
383	1.255	426	1.348
425	1.362	426	1.343
425	1.373	476	1.475
481	1.512	523	1.584
481	1.523	523	1.567
524	1.598	578	1.763
524	1.603	578	1.770
579	1.760	579	1.787
619	1.856	620	1.811
620	1.860	621	1.807

B. Experiments with higher CO_2 concentrations

After the experiments with trace concentrations the thermal diffusion factor for the mixtures 73.7 % He - 26.3 % CO_2, 51.6 % He - 48.4 % CO_2 and 20.4 % He - 79.6 % CO_2 was measured as a function of temperature and pressure. The results of the experiments are given in Table IV.4, 5 and 6, and plotted in Figs. 17, 18 and 19. For the 26.3 % CO_2 mixture the thermal diffusion factor is independent of temperature. For the other mixtures the α 's were obtained by drawing the tangent to the curves in Figs. 18 and 19 with a glass mirror ruler at integral values of T_2. The thermal diffusion factors of all the mixtures are given in Table IV.7.

The reproducibility in these experiments is not so good as with the trace concentrations; it is between 4 % for the 26.3 % CO_2 mixture and 6 % for the 79.6 % CO_2 mixture. For the 26.3 % CO_2 mixture the tangents of the straight lines through the measured points were calculated by the least squares method leading to an uncertainty in α of 4 %. For the other mixtures the error in the thermal diffusion factor is larger due to the uncertainty in the drawing of the tangent; the absolute value of the error can be 0.1.

TABLE IV.4

Experimental values of the separation factor for the system 73.7 % He - 26.3 % CO_2 at 28, 71 and 124 atm.

28 atm T_1 = 309 °K		71 atm T_1 = 308 °K		124 atm T_1 = 309 °K	
T_2 (°K)	Q	T_2 (°K)	Q	T_2 (°K)	Q
335	1.029	325	1.055	336	1.064
444	1.212	370	1.139	336	1.110
500	1.268	401	1.180	429	1.400
500	1.287	446	1.232	494	1.490
567	1.359	518	1.335	544	1.636
621	1.411	567	1.473	580	1.694
622	1.425	621	1.562	617	1.844

TABLE IV.5

Experimental values of the separation factor for the system 51.6 % He - 48.4 % CO_2 at 28, 72, 102 and 141 atm.

28 atm T_1 = 309 °K		72 atm T_1 = 311 °K		102 atm T_1 = 297 °K		141 atm T_1 = 309 °K	
T_2 (°K)	Q	T_2 (°K)	Q	T_2 (°K)	Q	T_2 (°K)	Q
333	1.035	335	1.029	326	1.133	336	1.191
386	1.121	379	1.211	369	1.354	387	1.611
435	1.192	429	1.349			436	1.936
438	1.196	471	1.391			487	2.116
485	1.260	535	1.512			533	2.231
533	1.323	574	1.558			617	2.358
571	1.392	616	1.601				
617	1.441						

TABLE IV.6

Experimental values of the separation factor for the system 20.4 % He - 79.6 % CO_2 at 26, 60 and 85 atm.

26 atm T_1 = 309 °K		60 atm T_1 = 310 °K		85 atm T_1 = 311 °K	
T_2 (°K)	Q	T_2 (°K)	Q	T_2 (°K)	Q
336	1.025	332	1.068	332	1.074 *)
376	1.107	375	1.270	371	1.356
430	1.201	427	1.412	425	1.556
495	1.269	475	1.508	470	1.782
537	1.308	522	1.587	479	1.877
538	1.283	570	1.646	526	1.940
577	1.305	617	1.730	570	1.939
624	1.283			620	2.011
				620	1.886

*) This value is too low; the convection through the upper ionization chamber did not work well.

TABLE IV.7

Experimental values of the thermal diffusion factor α for He - Kr and He - CO_2 mixtures at various concentrations, temperatures and pressures.

He with	$\sim$ 0% Kr		$\sim$ 0% CO_2		26.3% CO_2		
T (°C)	42 atm	135 atm	30 atm	134 atm	28 atm	71 atm	124 atm
75	0.83	0.82	0.92	0.88	0.52	0.62	0.85
150	0.83	0.82	0.92	0.88	0.52	0.62	0.85
225	0.83	0.82	0.92	0.88	0.52	0.62	0.85
300	0.83	0.82	0.92	0.53	0.52	0.62	0.85
He with	48.4% CO_2				79.6% CO_2		
T (°C)	28 atm	72 atm	102 atm	141 atm	26 atm	60 atm	85 atm
75	0.53	0.93	1.40	2.13	0.53	1.27	1.53
150	0.53	0.75	-	1.31	0.53	0.68	1.38
225	0.53	0.51	-	0.54	0.36	0.53	0.41
300	0.53	0.50	-	0.47	< 0.2	0.48	0.23

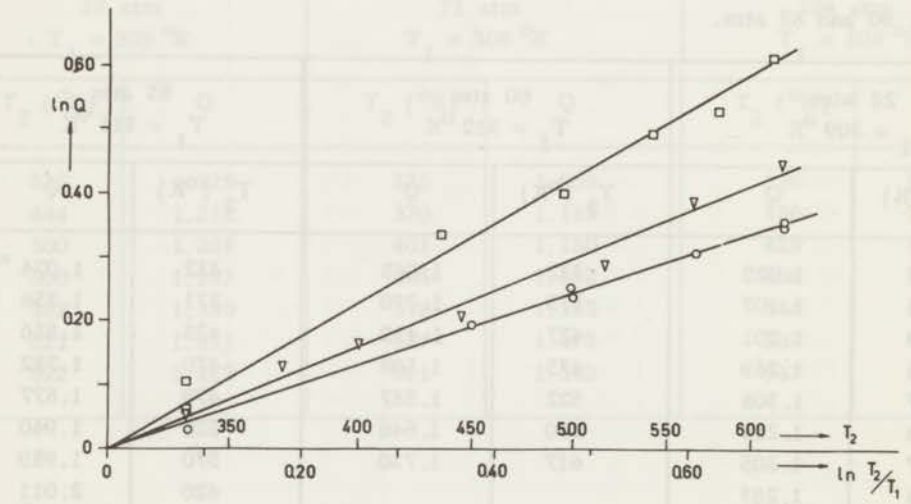

Fig. 17

Logarithm of the separation factor as a function of temperature for the system 73.7% He - 26.3% CO_2. ○ 28 atm ▽ 71 atm □ 124 atm

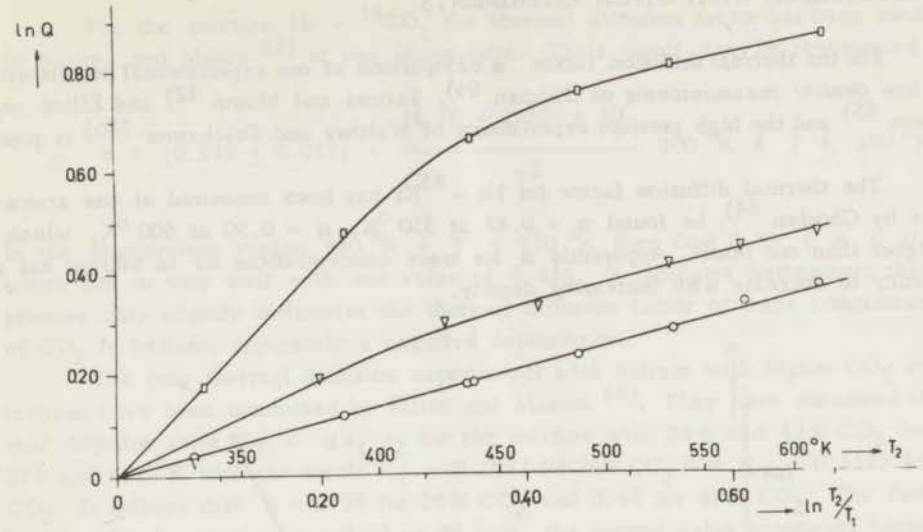

Fig. 18

Logarithm of the separation factor as a function of temperature for the system 51.6 % He - 48.4 % CO_2. ○ 28 atm ▽ 72 atm □ 141 atm.

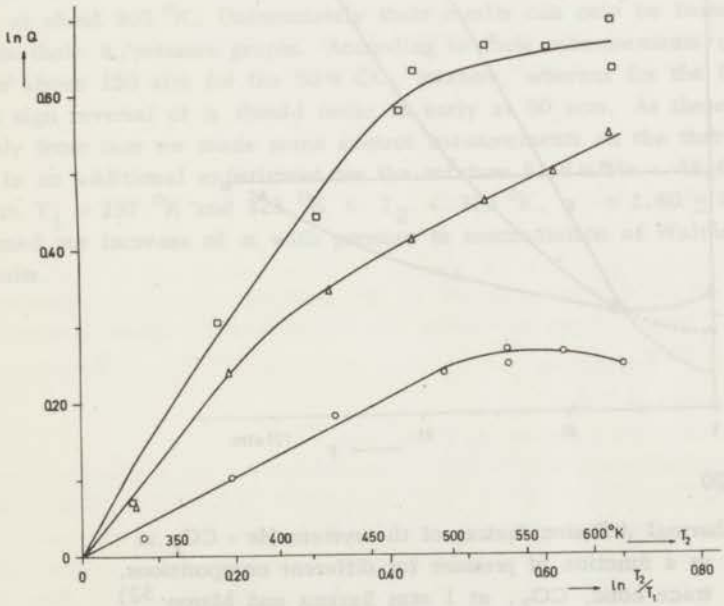

Fig. 19

Logarithm of the separation factor as a function of temperature for the system 20.4 % He - 79.6 % CO_2. ○ 26 atm △ 60 atm □ 85 atm.

5. COMPARISON WITH OTHER EXPERIMENTS

For the thermal diffusion factor α comparison of our experimental results with the low density measurements of Ghozlan [64], Saxena and Mason [32] and Elliot and Masson [65] and the high pressure experiments of Walther and Drickamer [12b] is possible.

The thermal diffusion factor for He - ^{85}Kr has been measured at one atmosphere by Ghozlan [64]; he found $\alpha = 0.87$ at 350 °K, $\alpha = 0.90$ at 600 °K, which is higher than our result. Apparently α for trace concentrations Kr in helium has a tendency to decrease with increasing density.

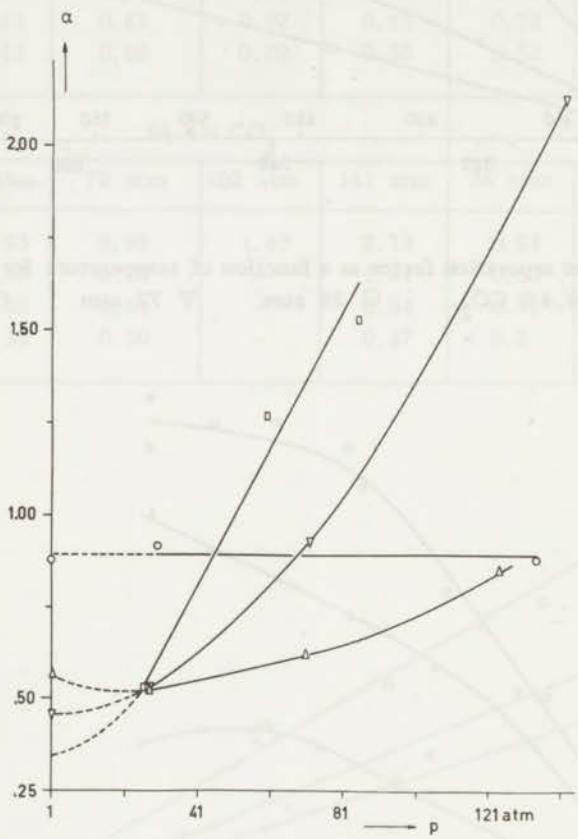

Fig. 20

The thermal diffusion factors of the system He - CO_2 at 75 °C as a function of pressure for different compositions.

- ○ trace conc. CO_2, at 1 atm Saxena and Mason [32]
- △ 26.3 % CO_2, at 1 atm Elliot and Masson [65]
- ▽ 48.4 % CO_2, at 1 atm Elliot and Masson [65]
- □ 79.6 % CO_2, at 1 atm theory Kihara [36]

For the mixture He - $^{14}CO_2$ the thermal diffusion factor has been measured by Saxena and Mason [32] at one atmosphere. Their result can be represented by:

$$\alpha = (0.918 \pm 0.017) - \frac{(4.70 \pm 1.32) \times 10^3}{T^2} \qquad 200\ ^{\circ}K \leqslant T \leqslant 530\ ^{\circ}K$$

In the temperature region $330\ ^{\circ}K < T < 620\ ^{\circ}K$ they find $0.88 \leqslant \alpha \leqslant 0.90$, which fits in very well with our value of 0.916. It indicates furthermore that the pressure only slightly influences the thermal diffusion factor of trace concentrations of CO_2 in helium; apparently a negative dependence.

The only thermal diffusion experiments with helium with higher CO_2 concentrations have been conducted by Elliot and Masson [65]. They have measured the thermal diffusion ratio $K_T = \alpha x_1 x_2$ for the mixture with 26% and 49% CO_2 between 273 and 492 °K with the result $K_T = 0.1087$ for 26% CO_2 and $K_T = 0.1135$ for 49% CO_2. It follows that $\alpha = 0.56$ for 26% CO_2 and 0.46 for 48% CO_2. The first value is somewhat larger than our 0.52 at 28 atm, the second value somewhat lower than our value at 28 atm. Figure 20 shows our experimental values for α at different concentrations as a function of pressure, together with the low pressure values of other authors.

Walther and Drickamer [12b] have measured the thermal diffusion factor between 100 and 1000 atm for the mixtures 50% CO_2 - 50% He and 80% CO_2 - 20% He at about 305 °K. Unfortunately their results can only be found by interpolation from their α/pressure graphs. According to their measurements α should be negative above 150 atm for the 50% CO_2 mixture, whereas for the 80% CO_2 mixture the sign reversal of α should occur as early as 50 atm. As these results deviate seriously from ours we made some control measurements on the thermal diffusion factor α in an additional experiment for the mixture 51.6% He - 48.4% CO_2 at 102 atm. With $T_1 = 297\ ^{\circ}K$ and $323\ ^{\circ}K < T_2 < 370\ ^{\circ}K$, $\alpha = 1.40 \pm 0.05$, which confirmed our increase of α with pressure in contradiction of Walther and Drickamer's results.

CHAPTER V

DISCUSSION OF THE EXPERIMENTAL RESULTS

1. COMPARISON OF THE EXPERIMENTS WITH THEORY

In this chapter the experiments will be compared with the theories outlined in chapter III. The most promising theories, those of Haase and the "fugacity" method, are discussed in extension; some of the results of the other theories will be given first.

The thermal diffusion factor has been calculated with Eq. (3.5) for He - CO_2 at various pressures. As Enskog's dense gas theory is based on the assumption that the molecules behave as rigid spheres, his values differ from the more refined Kihara approximation (Eq. 3.4) at 1 atm. From 1 - 150 atm, however, Enskog's theory predicts a decrease in α of 3 - 11 % dependent on the concentrations in the entire temperature range 323 - 623 °K. This decrease has not been found in the experiments. Drickamer et al [9b] have already reported that this theory fails to predict the thermal diffusion factor even qualitatively. Therefore, this theory will not be considered further here.

For the influence of the dimer formation on the thermal diffusion factor the number density of dimers must be known. The relation to the reduced equilibrium constant K^* is

$$\frac{n_2}{n_1^2} = \frac{2}{3} \pi \sigma_{12}^3 K^*$$

where n_1 and n_2 are the number densities of the monomer and dimer complex,
σ_{12} is the Lennard - Jones parameter for the monomer - dimer interaction
$\sigma_{dimer} = 1.02\, \sigma_{monomer}$ [60],
σ has been taken 4.1 Å,
K^* is tabulated as a function of T^* in ref. [60].

For CO_2 ε/k is approximately 200 °K which means that for the temperature range 300 °K < T < 630 °K, $1.5 < T^* < 3.2$ or $3.0 > K^* > 1.1$. The dimer concentration is temperature dependent, it decreases with increasing temperature. The largest dimer concentration can be expected at T = 300 °K; for a partial CO_2 pressure of 80 atm the calculation of the dimer concentration gives 35 %. Now the effective thermal diffusion factor $\alpha_{ij}^{(tern)}$ can be calculated for a ternary mixture with a total pressure of 160 atm and concentrations: monomer 32.5 % dimer 17.5 % and helium 50.0 %. After a lengthy calculation the result is an apparent increase of α by 0.12, or 25 %.

The maximum value for the correction term α' as a consequence of the enthalpy change by the dimer formation can be estimated as follows: The value $\Delta H/RT$ has been given in Stogryn's article [59] as a function of T^*. Between $T^* = 1.5$ and $T^* = 3.2$, $\Delta H/RT = -2.6$ to -2.5. When we ascribe $\alpha_d(1 - \alpha_d)$ its maximum value 0.25 it follows that $x_2/x_1 = 1.34$ and $\alpha'_{max} = 0.28$.

The influence of the clustering of CO_2 molecules on the thermal diffusion factor can be given by a correction to α of 0.3 maximum. This means that only part of the increase in α found in the experiments can be ascribed to dimer formation.

In order to calculate α numerically for Kotousov's formula an equation of state can be introduced into Eq. (3.15) by means of the thermodynamical relations:

$$H_i - H_i^{\circ} = -RT^2 \left(\frac{\partial \ln f_i}{\partial T}\right)_{p,x} \tag{5.1}$$

$$\ln f_i = \ln x_i + \ln p - \frac{1}{RT} \int_0^p \left(\frac{RT}{p} - V_i\right) dp$$

The drawback of Kotousov's expression is that values for λ and D_{12} at high pressure are required. Therefore, we first evaluate his equation for low densities. When the virial equation of state $pV = RT + B(T)\,p$ is used:

$$V_i = \frac{RT}{p} + B_{ii} + (1 - x_i)^2 \Delta ,$$

with $B(T) = B_{11} x_1^2 + 2 B_{12} x_1 x_2 + B_{22} x_2^2$, the second virial coefficient for a mixture,

B_{ii} = the second virial coefficient for the pure component,

$\Delta \equiv 2 B_{12} - B_{11} - B_{22}$.

Consequently Eq. (3.15) becomes:

$$\alpha = \frac{2\left(\Delta - T \frac{\partial \Delta}{\partial T}\right)}{T\left[\frac{\partial^2 B_{11}}{\partial T^2} - \frac{\partial^2 B_{22}}{\partial T^2} + (x_2 - x_1)\frac{\partial^2 \Delta}{\partial T^2}\right]} \frac{\lambda}{\rho D_{12}} \frac{M}{RT - 2p x_1 x_2 \Delta}$$

The equation can be developed theoretically by means of the B coefficients as tabulated in Hirschfelder's book [18] for the Lennard - Jones (12 - 6) model. The result of the calculation for a mixture of 48.4% CO_2 - 51.6% He at 461 °K is $\alpha = 0.0023$.

This is some orders of magnitude smaller than the experiments and other theories show.

The pressure dependence comes into the equation through the factors $\lambda / \rho D_{12}$ and $RT - 2p x_1 x_2 \Delta$. The latter factor changes 45 % between 1 and 150 atm. The results of experiments on thermal conductivity measurements at elevated gas densities made by Franck [66] and Sengers [67] have shown that λ_{He} does not appreciably vary between 1 and 144 atm, but that λ_{CO_2} can increase by 350 %. It means that at 144 atm α is certainly less than 0.01, which does not fit in with the experiments. No further calculations have been made with Kotousov's formula.

To obtain numerical results with Haase's theory and the "fugacity" method the quantities h and f must be known. They can be calculated from an equation of state. To compare the theories and the equations of state the "fugacity" method has been calculated using the Van der Waals equation of state and a simplified Beattie - Bridgeman equation, whereas Haase's theory has been evaluated with the Beattie - Bridgeman equation of state. This equation has been simplified as follows:

$$pV = RT + B(T)\,p.$$

For a mixture $B(T) = B_{11} x_1^2 + 2 B_{12} x_1 x_2 + B_{22} x_2^2$, with B_{ii} the second virial coefficient for the pure component, according to Beattie and Bridgeman [68]:

$$B_{ii} = (B_o)_{ii} - \frac{(A_o)_{ii}}{RT} - \frac{c_{ii}}{T^3} .$$

A_o, B_o and c are constants for which the following combination laws are valid:

$$(A_o)_{12} = \sqrt{(A_o)_{11} \cdot (A_o)_{22}} \qquad c_{12} = \sqrt{c_{11} \cdot c_{22}}$$

$$(B_o)_{12} = \frac{1}{8} \left[\sqrt[3]{(B_o)_{11}} + \sqrt[3]{(B_o)_{22}} \right]^3 .$$

For the simplified Beattie - Bridgeman equation:

$$\ln f_i = \ln p x_i + \frac{B_{ii}\, p}{RT} + \frac{p (1 - x_i)^2 \Delta}{RT}$$

with $\Delta = 2 B_{12} - B_{11} - B_{22}$. As a consequence Eq. (3.17) is:

$$\ln Q_{real} = \frac{p}{R} \left\{ \frac{B_{11c} - B_{22c} + (x_2 - x_1)\,\Delta_c}{T_1} - \frac{B_{11h} - B_{22h} + (x_2 - x_1)\,\Delta_h}{T_2} \right\} \qquad (5.2)$$

The Beattie - Bridgeman constants that have been used are given in Table V.1.

TABLE V.1

Van der Waals and Beattie - Bridgeman constants for helium, CO_2 and the He - CO_2 mixture.

	Van der Waals constants		Beattie - Bridgeman constants		
gas	a $\frac{\text{litres}^2 \text{ at}}{\text{mole}^2}$	b litres/mole	A_o $\frac{\text{litres}^2 \text{ at}}{\text{mole}^2}$	B_o litres/mole	c $\frac{\text{litres } {}^oK^3}{\text{mole}}$
He	0.034	2.38×10^{-2}	0.0216	0.014	0.004×10^4
CO_2	3.60	4.28×10^{-2}	5.0065	0.10476	66×10^4
He - CO_2	0.35	3.25×10^{-2}	0.3288	0.0451	0.514×10^4

For the Van der Waals equation of state:

$$\ln f_i = \ln \frac{x_i R T}{V - b} + \frac{B_i}{V - b} - \frac{A_i}{V R T} \qquad (5.3)$$

with: $a = a_{11} x_1^2 + 2 a_{12} x_1 x_2 + a_{22} x_2^2$

$b = b_{11} x_1^2 + 2 b_{12} x_1 x_2 + b_{22} x_2^2$

$a_{12} = \sqrt{a_{11} \cdot a_{22}}$ $\qquad b_{12} = \frac{1}{8} \left[\sqrt[3]{b_{11}} + \sqrt[3]{b_{22}} \right]^3$

a_{ii} and b_{ii} are the constants for the pure component

A_i and B_i are defined by:

$A_1 = 2 (a_{11} x_1 + a_{12} x_2)$ $\qquad B_1 = b_{11} - x_2^2 (b_{11} - 2 b_{12} + b_{22})$

and cyclic interchange.

The universal equation (3.17) now becomes:

$$\ln \left(\frac{x_1}{x_2}\right)_h - \ln \left(\frac{x_1}{x_2}\right)_c = \ln Q_{real} = \frac{(B_1 - B_2)(V_h - V_c)}{(V_c - b)(V_h - b)} + \frac{(A_1 - A_2)(T_1 V_c - T_2 V_h)}{R T_1 T_2 V_c V_h} \qquad (5.4)$$

The values used for the Van der Waals constants are given in Table V.1.

For the "fugacity" method numerical calculations have been made on an ELX1 computer (N.V. Electrologica, The Hague) giving the separation as a function of pressure, composition and T_2 . T_1 has been taken constant at 309 °K.

Two comments should be made:

1. When solving for $\ln Q_{real}$ from (5.2) and (5.4) one has to take into account that A_i, B_i and b are concentration dependent so that they vary with temperature. In Eq. (5.2) the unknown x_1 and x_2 also appear on the right hand side. The equations can then be solved only by expanding the logarithm or by a trial and error procedure. In a first approximation we have given the x_i at the right hand side the values at 309 °K. After the calculation an estimation of the error can be made. It was found that B_i changed less than 0.1% and b less than 8%, but A_i could vary 19% in the worst case (48.4% CO_2 - 51.6% He at 141 atm). Therefore, in the second approximation we have distinguished between A_{ic} and A_{ih} and have given them their values for x_{ic} and x_{ih} .

2. From the separation in the gas mixture at the temperature gradient the factor $\bar{\alpha}_{real} = \dfrac{\ln Q}{\ln T_2/T_1}$ can be calculated. This α_{real} is an average value for the temperature region T_1 to T_2. It must be distinguished from the method by Haase that gives a separation at a specified temperature T.

In order to calculate α numerically according to Haase the equation of state can be introduced into (3.14) through the relations (5.1). For the simplified Beattie-Bridgeman equation:

$$H_i - H_i^{o} = p \left[B_{ii} - T \frac{\partial B_{ii}}{\partial T} + (1 - x_i)^2 \left(\Delta - T \frac{\partial \Delta}{\partial T} \right) \right]$$

which shows a linear dependence of α on pressure. Eq. (3.14) becomes:

$$\alpha = \frac{MRT\alpha_o + p \left[M_1 \left(B_{22} - T \frac{\partial B_{22}}{\partial T} \right) - M_2 \left(B_{11} - T \frac{\partial B_{11}}{\partial T} \right) + \left(M_1 x_1^{\,2} - M_2 x_2^{\,2} \right) \left(\Delta - T \frac{\partial \Delta}{\partial T} \right) \right]}{M \left(RT - 2 p x_1 x_2 \Delta \right)} \qquad (5.5)$$

This equation gives the total thermal diffusion factor α for a fixed temperature T. With (5.5) α has been calculated for different compositions of the He - CO_2 mixture, as a function of p and T, using the Beattie - Bridgeman virial coefficients. To compare the theory with the experiments the separation factor Q has been calculated as

$$\ln Q = \int_{T_1}^{T_2} \alpha \ln T.$$

As numerical results of Eq. (5.5) show that α is temperature dependent, ln Q can only be found by a numerical integration of α ln T between T_1 and T_2.

Table V.2 shows the experimental separation factor ln Q, the theoretical value of ln Q at 1 atm, the difference between these two Δ ln Q and the separation factors owing to the non-ideality of the gas mixture according to Eqs. (5.2), (5.4) and (5.5). The values for $T_2 = 617\ ^{o}K$ have been plotted as a function of pressure in Figs. 21 - 24.

The concentrations given in Table V.2 are initial values. It is also the composition in the connecting tube half-way between hot and cold reservoir at the end of an experiment when the volumes of both reservoirs are equal or when the separation is small. This mean concentration changes, however, when the bulbs are not of the same size. For large separations as with the 48.4% CO_2 - 51.6% He mixture at 141 atm the mean CO_2 concentration can change to 46.3% CO_2. A correction has to be made for this effect.

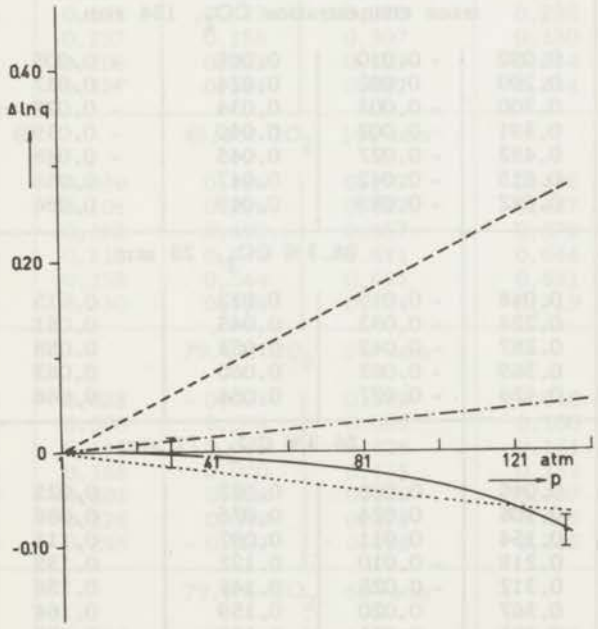

Fig. 21

Reality contribution to the logarithm of the separation factor, both experimental and theoretical, as a function of pressure, for a temperature difference of 308°, for trace concentrations CO_2 in helium $T_1 = 309\ ^{o}K$ $T_2 = 617\ ^{o}K$
——— experimental ..... fugacity Beattie - Bridgeman
------ Haase's theory -.-.-. fugacity Van der Waals.

TABLE V.2

Comparison between the logarithm of the experimental and theoretical separation factors above the values at 1 atm.

T_2	ln Q experimental	ln Q 1 atm theoretical	Δ ln Q experimental	Δ ln Q fugacity v.d.Waals	Δ ln Q fugacity Beattie-Bridgeman	Δ ln Q Haase Beattie-Bridgeman
		trace concentration CO_2, 30 atm				
330	0.092	0.088	0.004	0.002	- 0.001	0.012
382	0.224	0.213	0.011	0.007	- 0.004	0.027
425	0.313	0.307	0.006	0.009	- 0.006	0.035
481	0.417	0.405	0.012	0.011	- 0.009	0.044
524	0.471	0.480	- 0.009	0.012	- 0.011	0.049
579	0.565	0.563	0.002	0.013	- 0.013	0.054
619	0.620	0.621	- 0.001	0.013	- 0.015	0.058
		trace concentration CO_2, 134 atm				
330	0.082	0.092	- 0.010	0.008	- 0.005	0.058
381	0.202	0.200	0.002	0.024	- 0.017	0.115
426	0.297	0.300	- 0.003	0.034	- 0.027	0.157
476	0.389	0.391	- 0.002	0.040	- 0.039	0.193
523	0.455	0.482	- 0.027	0.045	- 0.048	0.221
578	0.573	0.615	- 0.042	0.047	- 0.058	0.259
620	0.593	0.682	- 0.089	0.049	- 0.066	0.275
			26.3 % CO_2, 28 atm			
335	0.029	0.048	- 0.019	0.012	0.015	0.018
444	0.192	0.224	- 0.032	0.045	0.051	0.063
500	0.245	0.287	- 0.042	0.053	0.058	0.074
567	0.307	0.369	- 0.062	0.060	0.063	0.079
621	0.349	0.426	- 0.077	0.064	0.066	0.081
			26.3 % CO_2, 71 atm			
325	0.054	0.046	0.008	0.022	0.025	0.047
370	0.130	0.106	0.024	0.076	0.086	0.091
401	0.165	0.154	0.011	0.097	0.111	0.118
446	0.208	0.218	- 0.010	0.122	0.135	0.151
518	0.289	0.312	- 0.023	0.148	0.156	0.176
567	0.387	0.367	0.020	0.159	0.164	0.193
621	0.446	0.425	0.021	0.169	0.170	0.203
			26.3% CO_2, 124 atm			
336	0.083	0.047	0.036	0.065	0.078	0.109
429	0.336	0.205	0.131	0.207	0.233	0.323
494	0.399	0.281	0.118	0.254	0.272	0.388
544	0.492	0.342	0.150	0.277	0.288	0.418
580	0.527	0.383	0.144	0.290	0.296	0.440
617	0.612	0.419	0.193	0.318	0.302	0.454

TABLE V.2 (continued)

T_2	ln Q experimental	ln Q 1 atm theoretical	Δ ln Q experimental	Δ ln Q fugacity v. d. Waals	Δ ln Q fugacity Beattie-Bridgeman	Δ ln Q Haase Beattie-Bridgeman
			48.4 % CO_2, 28 atm			
333	0.035	0.034	0.001	0.020	0.027	0.024
386	0.114	0.100	0.014	0.057	0.073	0.061
437	0.177	0.161	0.016	0.079	0.098	0.082
485	0.231	0.210	0.021	0.093	0.113	0.096
533	0.280	0.259	0.021	0.103	0.123	0.106
571	0.331	0.292	0.039	0.109	0.129	0.113
617	0.365	0.328	0.037	0.115	0.134	0.118
			48.4 % CO_2, 72 atm			
335	0.029	0.034	- 0.005	0.074	0.083	0.072
379	0.191	0.090	0.101	0.173	0.194	0.161
429	0.299	0.150	0.149	0.236	0.263	0.224
471	0.330	0.193	0.137	0.270	0.298	0.260
535	0.413	0.257	0.156	0.307	0.330	0.298
574	0.443	0.290	0.153	0.323	0.344	0.315
616	0.471	0.327	0.144	0.337	0.354	0.329
			48.4 % CO_2, 141 atm			
336	0.175	0.039	0.136	0.177	0.196	0.211
387	0.477	0.101	0.376	0.427	0.457	0.450
436	0.661	0.162	0.499	0.557	0.576	0.582
487	0.750	0.212	0.538	0.641	0.644	0.663
533	0.802	0.258	0.544	0.691	0.681	0.712
617	0.858	0.330	0.528	0.751	0.719	0.772
			79.6 % CO_2, 26 atm			
336	0.025	0.028	- 0.003	0.039	0.048	0.031
376	0.102	0.068	0.034	0.086	0.106	0.065
430	0.183	0.118	0.065	0.126	0.151	0.095
495	0.238	0.168	0.070	0.155	0.183	0.117
537	0.259	0.201	0.058	0.168	0.197	0.127
577	0.266	0.226	0.040	0.178	0.206	0.134
624	0.249	0.256	- 0.007	0.186	0.215	0.140
			79.6 % CO_2, 60 atm			
332	0.066	0.024	0.042	0.107	0.105	0.065
375	0.239	0.066	0.173	0.273	0.267	0.155
427	0.345	0.115	0.230	0.382	0.371	0.221
475	0.411	0.153	0.258	0.444	0.428	0.263
522	0.462	0.190	0.272	0.486	0.464	0.291
570	0.499	0.222	0.277	0.516	0.490	0.313
617	0.548	0.249	0.299	0.537	0.507	0.328

TABLE V.2 (continued)

T_2	ln Q experimental	ln Q 1 atm theoretical	Δln Q experimental	Δln Q fugacity v.d. Waals	Δln Q fugacity Beattie-Bridgeman	Δln Q Haase Beattie-Bridgeman
			79.6 % CO_2, 85 atm			
332	0.071	0.023	0.048	0.199	0.159	0.093
371	0.305	0.061	0.244	0.485	0.389	0.221
425	0.442	0.109	0.333	0.672	0.546	0.328
470	0.578	0.148	0.430	0.763	0.621	0.392
479	0.630	0.154	0.476	0.776	0.630	0.402
526	0.663	0.190	0.473	0.836	0.672	0.442
570	0.662	0.219	0.443	0.876	0.700	0.471
620	0.698	0.251	0.447	0.910	0.724	0.497

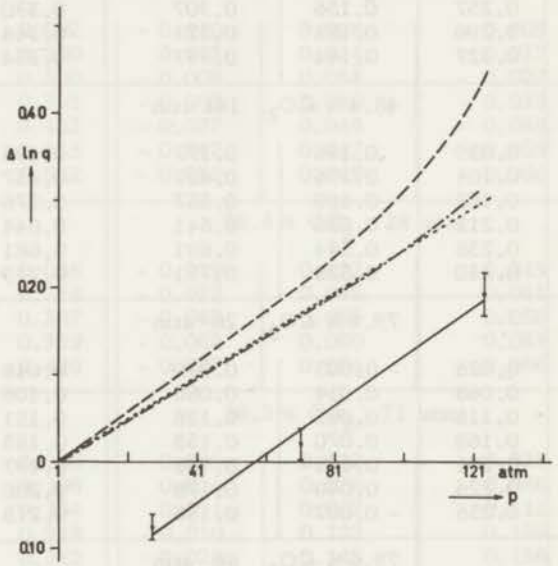

Fig. 22

Reality contribution to the logarithm of the separation factor, both experimental and theoretical, as a function of pressure, for a temperature difference of 308°, for the system 73.7 % He - 26.3 % CO_2 T_1 = 309 °K T_2 = 617 °K

_____ experimental ..... fugacity Beattie - Bridgeman

------ Haase's theory -.-.-. fugacity Van der Waals.

2. DISCUSSION

The data plotted in Figs. 20 - 24 show that in general the experimental values for the separation and the thermal diffusion factor increase with increasing pressure. For trace concentrations CO_2, as well as Kr, however, the thermal diffusion factor is constant or has a tendency to decrease with pressure at high temperature. The pressure dependence of α between 1 atm and 20 atm is negligible. To design a thermal diffusion column for concentration of impurities in helium at 20 atm the low density value of α can be used.

For the mixtures with 48.4 % and 79.6 % CO_2 the pressure dependence of α is pronounced at 75 °C but considerably less at 300 °C. It may be due to the critical point of CO_2 which is 31 °C and 73 atm. Walther's experiments [12b] also indicate that at the critical density of one of the components large effects in α can occur.

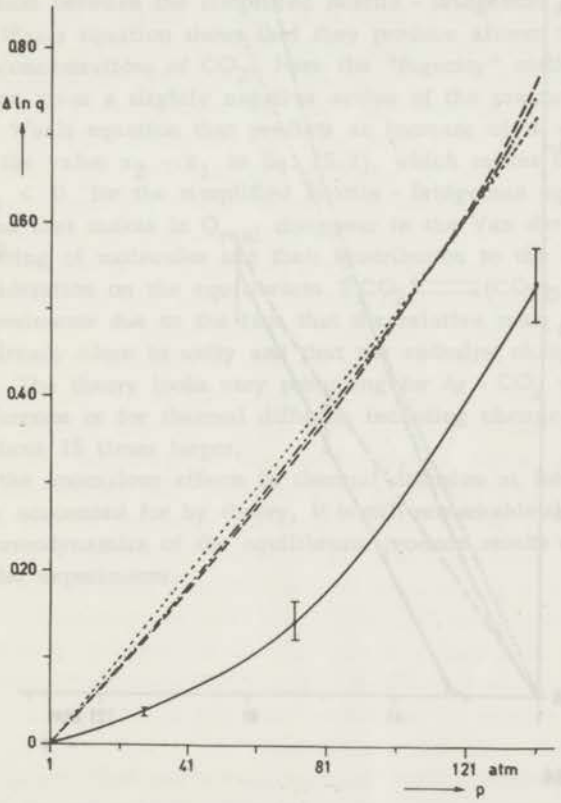

Fig. 23

Reality contribution to the logarithm of the separation factor, both experimental and theoretical, as a function of pressure, for a temperature difference of 308°, for the system 51.6 % He - 48.4 % CO_2 $T_1 = 309$ °K $T_2 = 617$ °K

——— experimental ..... fugacity Beattie - Bridgeman

------ Haase's theory -.-.-. fugacity Van der Waals.

So far as theory is concerned, the kinetic theory does not yet give explicit expressions for the thermal diffusion factor. A simplification of this theory (Enskog) yields results which contradict the experiments (Sec. V.1; Drickamer [9b]).

The theory of thermodynamics of irreversible processes predicts only the relationships between the transport coefficients. With an assumption outside the scope of thermodynamics Haase succeeded to derive a formula that gives the pressure dependence of α as a consequence of the non-ideality of the gas.

The "fugacity" method is based on the non-ideality of the gas mixture and predicts a separation in a temperature gradient as a consequence of this property.

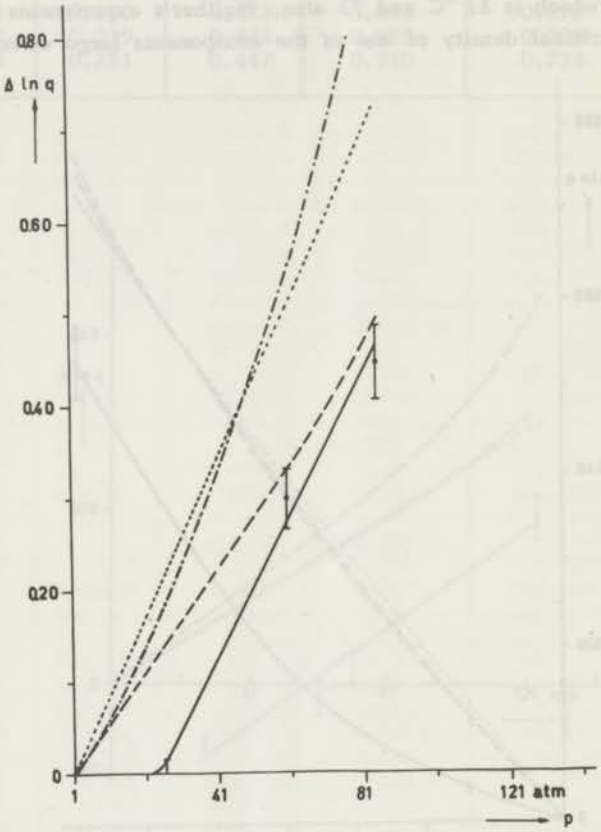

Fig. 24

Reality contribution to the logarithm of the separation factor, both experimental and theoretical, as a function of pressure, for a temperature difference of 308°, for the system 20.4 % He - 79.6 % CO_2 $T_1 = 309\ ^oK$ $T_2 = 617\ ^oK$
_____ experimental ..... fugacity Beattie - Bridgeman
------ Haase's theory -.-.-. fugacity Van der Waals.

Although Haase's theory and the "fugacity" method differ in their derivation they both predict qualitatively an increase of the separation with increasing pressure. This effect is more pronounced in higher CO_2 concentrations. Both theories give in first order a linear relation between the reality contribution and the pressure. At the highest pressure $\Delta \ln Q$ increases with a higher power of the pressure as a consequence of the factor $RT - 2 p x_1 x_2 \Delta$ in the denominator of Eq. (5.5). The experimental values are much lower than the theoretical at low pressure but they approach them at the highest pressure.

A difference between Haase's theory and the "fugacity" treatment turns up at low CO_2 concentration, which is a consequence of the concentration - dependent factor M in Eq. (3.18). The difference is especially striking for trace concentration CO_2, where Haase predicts an increase of α with pressure, whereas the experiments have a tendency to decrease with pressure.

A comparison between the simplified Beattie - Bridgeman equation of state and the Van der Waals equation shows that they produce almost the same results, except for trace concentrations of CO_2. Here the "fugacity" method with the Beattie-Bridgeman equation gives a slightly negative action of the pressure on α in contrast with the Van der Waals equation that predicts an increase of α with pressure. It is possible to solve the value $x_2 - x_1$ in Eq. (5.2), which makes $\ln Q_{real}$ zero. Below 2 % CO_2 $\ln Q_{real} < 0$ for the simplified Beattie - Bridgeman equation. No value for x can be found that makes $\ln Q_{real}$ disappear in the Van der Waals equation.

The clustering of molecules and their contribution to the increase of α follows from a consideration on the equilibrium $2\,CO_2 \rightleftarrows (CO_2)_2$. The effect is small for our experiments due to the fact that the relative mass difference between He and CO_2 is already close to unity and that the enthalpy change by the dimer formation is low. The theory looks very promising for Ar - CO_2 which has not such a large mass difference or for thermal diffusion including chemical reactions [62], where ΔH is about 15 times larger.

Although the anomalous effects in thermal diffusion at intermediate pressures are not rigorously accounted for by theory, it is still remarkable that treatments based essentially on thermodynamics of the equilibrium produce results which are in general agreement with the experiments.

SUMMARY

This thesis concerns some aspects of thermal diffusion at a moderately high pressure in both a two-bulb apparatus and a thermal diffusion column. In the first part a concentric cylinder column for concentrating trace quantities of CO_2 in helium gas at 20 atm pressure with a factor of at least 100 is described.

Chapter I deals with the theory of the thermal diffusion column. The equations of Jones and Furry, Fleischmann and Jensen, and Slieker for concentric cylinder column parameters are compared. They differ mostly when the deviation from the parallel plates type is greatest. The requirement that the flow in the column must be laminar means that it cannot work at optimum performance.

A stainless steel thermal diffusion column has been constructed, which is capable of enriching CO_2 in helium at 20 atm with a factor of 100 in 5 - 8 hours. The column - 100 cm long - has a large upper reservoir so as to keep the CO_2 concentration as constant as possible. Originally, the analysis was made with an infra-red gas analyser, but as this instrument has a few disadvantages when used at high pressure, we switched to $^{14}CO_2$ as trace component and ionization chambers for detecting it. In order to reduce the effects of adsorbing and desorbing CO_2 molecules on the cold wall experiments were carried out at a higher overall column temperature. Agreement between theory and experiment is poor, especially at low Reynolds numbers. An imperfection in the construction of the column has less influence on the initial transport than the stationary state separation. For the column operated with bleed-off comparison of experiment with theory is quite good.

Chapter III reviews the existing theories of transport phenomena at high density. The theory based on statistical mechanics, such as the distribution function method and the time correlation method, does not yet provide explicit expressions for the thermal diffusion factor. Enskog's dense gas correction on the Boltzmann equation leads to a slight decrease of α with pressure. The thermodynamics of irreversible processes developed by De Groot, Haase and Kotousov involve a quantity q_1^*, the heat of transfer, which can only be evaluated by making assumptions. Becker predicts separation in a gas mixture in a temperature gradient due to the non-ideality of one of the components. His theory has been supplemented to include all interactions, considering the equality of the ratio of the fugacity of both components at different temperatures. Another effect that can influence the thermal diffusion factor is the formation of clusters of molecules. How this clustering can contribute to an increase of α in three ways has been shown.

Chapter IV presents a short description of a two-bulb apparatus to measure the elementary effect up to 150 atm. Some calibration values of the analysing instruments (ionization chambers) are also given. The binary systems ^{85}Kr - He and $^{14}CO_2$ - He were measured up to 135 atm from 300 to 620 ^{o}K. Within the experimental accuracy only a slight decrease of α with pressure could be found for $^{14}CO_2$ - He. The pressure dependence of α was also measured for He - CO_2 mixtures with 26.3 %, 48.4 % and 79.6 % CO_2. Samples were taken and analysed in a mass spectrometer. All mixtures showed a large increase of α with pressure especially at tem-

peratures somewhat above room temperature.

A comparison of theory and experiment is made in chapter V. The formation of clusters can contribute to an increase of α by a maximum of 0.3. Kotousov's equation differs by several orders of magnitude from theory and experiment at 1 atm. His formula cannot be evaluated easily at high densities because it contains the heat conductivity and the diffusion coefficients. Haase's theory is treated numerically for a virial equation of state, whereas results for the fugacity method have been obtained with the Van der Waals equation of state and the virial equation. Both theories predict qualitatively an increase in the separation with pressure. Haase's theory differs from the fugacity method with a concentration-dependent factor $M = M_1 x_1 + M_2 x_2$. This matters especially at low CO_2 concentrations, where Haase's equation gives a large increase of α with pressure, which has not been found experimentally. In general the experimental values are much lower than theory at low pressure, but they approach it at the highest pressure. Although the anomalous effects in thermal diffusion at intermediate pressures are not fully explained by theory, it is still worthy of note that treatments based essentially on equilibrium thermodynamics produce results in general agreement with the experiments.

SAMENVATTING

Dit proefschrift belicht enige aspecten van thermodiffusie bij gematigd hoge drukken in een twee-bollen apparaat, zowel als in een thermodiffusie kolom. In het eerste deel wordt een beschrijving gegeven van een concentrische cylinder kolom om sporen concentraties CO_2 in helium bij 20 atm druk met tenminste een factor honderd te verrijken.

In hoofdstuk I wordt de theorie van de thermodiffusie kolom behandeld. De vergelijkingen van Jones en Furry, Fleischmann en Jensen en Slieker voor de concentrische cylinder kolom worden vergeleken. Het verschil tussen deze vergelijkingen is groter naarmate de afwijking van evenwijdige vlakke platen groter is. De voorwaarde dat de stroming in de kolom laminair moet zijn heeft tot gevolg dat hij niet onder optimale omstandigheden kan werken.

Er werd een roestvrij stalen kolom ontworpen in staat om CO_2 in helium bij 20 atm met een factor honderd te verrijken in 5 à 8 uur. De kolom, die 100 cm lang is, heeft een groot bovenvolume om de concentratie zo goed mogelijk constant te houden. Oorspronkelijk werd de analyse uitgevoerd met een infrarood gasanalysator, maar daar dit instrument enige nadelen heeft bij gebruik op hoge druk gingen wij over op $^{14}CO_2$ en ionisatiekamers als detectoren. Om het effect van adsorptie en desorptie van CO_2 moleculen aan de koude wand te verminderen, werden experimenten gedaan met een hoge temperatuur van de koelmantel. De overeenstemming tussen theorie en experiment is slecht, vooral bij lage Reynoldsgetallen. Onvolkomenheden in de constructie van de kolom beïnvloeden het begintransport minder dan de uiteindelijke scheiding. Voor de kolom met aftap is de overeenkomst tussen experiment en theorie goed.

In hoofdstuk III wordt een overzicht gegeven van de bestaande theorieën over transportverschijnselen bij hogere dichtheid. De theorie gebaseerd op de statistische mechanica, zoals de verdelingsfunctie-methode en de correlatiefunctie-methode geven nog geen uitgewerkte vergelijkingen voor de thermodiffusiefactor. Enskogs correcties voor een verdicht gas op de Boltzmann vergelijking leveren een kleine afname van α met de druk op. Een methode volgens de lijnen van de thermodynamica der irreversibele processen ontwikkeld door de Groot, Haase en Kotousov bevat een grootheid q_1^*, de overgangswarmte, die slechts ontwikkeld kan worden door het maken van diverse veronderstellingen. Becker voorspelt een scheiding in een gasmengsel in een temperatuurgradiënt tengevolge van het niet-ideaal zijn van een van de componenten. Zijn theorie wordt hier verder uitgewerkt, waarbij alle interacties in beschouwing worden genomen, door de verhouding van de fugaciteit van beide componenten bij verschillende temperaturen aan elkaar gelijk te stellen. Een ander verschijnsel dat de thermodiffusiefactor kan beïnvloeden is de vorming van clusters van moleculen. Er wordt aangetoond hoe deze clustervorming op drie manieren aan een toename van α kan bijdragen.

In hoofdstuk IV wordt een twee-bollen apparaat beschreven waarmee het elementaire thermodiffusie effect tot 150 atm is gemeten. Hierbij wordt ook aandacht besteed aan de ijking van de ionisatiekamers, die als analyse-instrument werden ge-

bruikt. De binaire systemen ^{85}Kr - He en $^{14}CO_2$ - He zijn gemeten tot 135 atm tussen 300 en 620 ^{o}K. Binnen de experimentele foutengrens werd een kleine afname van α met de druk gevonden voor $^{14}CO_2$ - He. Daarna werd de drukafhankelijkheid van α bepaald voor He - CO_2 mengsels met 26,3 %, 48,4 % en 79,6 % CO_2. Hierbij werden monsters getrokken en geanalyseerd in een massaspectrometer. Alle mengsels vertoonden een grote toename van α met de druk, vooral bij temperaturen dicht boven kamertemperatuur.

In hoofdstuk V worden de experimenten met de theorie vergeleken. De vorming van clusters kan een toename van α met maximaal 0.3 tengevolge hebben. Kotousovs formule levert een α die enige grootte-orden te laag is bij 1 atm vergeleken met andere theorieën en experimenten. Voor hogere dichtheden kan zijn formule niet gemakkelijk worden uitgewerkt daar deze de warmtegeleiding en de diffusiecoëfficiënt bevat. Numerieke resultaten zijn verkregen voor de theorie van Haase met behulp van een viriaal toestandsvergelijking en voor de fugaciteitenmethode met de Van der Waals vergelijking en de viriaalvergelijking. Beide theorieën voorspellen kwalitatief een toename van de scheiding met de druk. Het verschil tussen Haases theorie en de fugaciteitenmethode zit in een concentratie-afhankelijke factor $M = M_1 x_1 + M_2 x_2$. Deze is vooral belangrijk bij lage CO_2 concentraties. Haases formule geeft hier een grote toename van α met de druk die experimenteel niet is gevonden. In het algemeen blijven de experimentele waarden achter bij de theorie, vooral bij lage druk, maar ze naderen die bij de hoogste drukken. Ofschoon de optredende effecten in thermodiffusie bij gematigd hoge drukken niet volkomen door de theorie worden verklaard, blijft het toch opmerkelijk dat beschouwingen die essentieel zijn gebaseerd op de thermodynamica van evenwichtsprocessen, resultaten geven die in het algemeen overeenstemmen met experimenten over transportverschijnselen.

LIST OF SYMBOLS

The numbers indicate the pages on which the symbols are introduced.

a	ratio of inner radius over outer radius r_h/r_c,	5
a	virial coefficient in the Van der Waals equation of state,	41
b	co-volume in the Van der Waals equation of state,	41
$c_1 \ldots c_6$	column parameters according to Cohen,	2
c_7	cascade parameter for parasitic currents,	14
$\vec{c}$	linear velocity of the mass centre of a molecule,	35
c_{ii}	coefficient in the equation of state of Beattie - Bridgeman,	64
c_i	concentration of component i (mass fraction),	39
c_p	heat capacity at constant pressure,	12
d	distance between hot wall and cold wall in a column,	4
e	base of natural logarithms,	5
$f(\vec{c}, \vec{r})$	velocity distribution function,	32
f	fugacity,	40
f_i	fugacity of component i in a mixture,	42
g	gravitational acceleration,	4
h_i	partial specific enthalpy of component i,	39
k	Boltzmann's constant,	34
$\vec{k}$	unit vector,	35
m	ratio p^2/p^2_{opt},	8
$n(\vec{r}, t)$	local particle density,	34
n_i	number density of molecules of component i,	37
p	pressure,	1
p_{opt}	optimum pressure,	8
q	enrichment in a thermal diffusion column: Nz/No,	5
q_1^*	heat of transfer,	38
r	radial coordinate,	4

r_c, r_h	radius of cold and hot cylinder,	4
r_m	distance of the minimum of the Lennard - Jones potential field,	33
s_i	partial specific entropy of component i,	39
t	time,	2
t_r	relaxation time in a thermal diffusion experiment,	11
$\vec{u}(\vec{r}, t)$	local average velocity,	34
v	convection velocity in axial direction in a column,	4
$\vec{v}$	centre of mass velocity,	38
$\vec{v_i}$	velocity of component i,	38
v_i	partial specific volume of component i,	39
x	horizontal coordinate,	4
x_i	mole fraction of component i,	33
z	vertical coordinate,	2
A	cross-sectional area of thermal diffusion tube,	52
A^*	ratio of two collision integrals,	13
$(Ao)_{ii}$	coefficient in the equation of state of Beattie - Bridgeman,	64
B	mean circumference of thermal diffusion column,	4
B^*	ratio of collision integrals,	37
$(Bo)_{ii}$	coefficient in the equation of state of Beattie - Bridgeman,	64
B (T)	second virial coefficient,	63
C^*	ratio of two collision integrals,	34
D	self-diffusion coefficient,	4
D_{12}	diffusion coefficient of binary mixture,	1
D_T	thermal diffusion coefficient,	1
E	heat input,	17
GrPr	Grashof - Prandtl number,	12
H	mass of gas in positive reservoir,	5
H'	mass of gas in negative reservoir,	11
$H_{eff.}$	effective mass of gas in positive reservoir,	30
H_i	partial molar enthalpy of component i,	41

I	ionization current,	49
$\vec{J}$, $\vec{J}_i$	flux of matter of component i,	1
$\vec{J}_q$	heat flux,	37
K^*	reduced equilibrium constant for dissociation,	44
K_p	equilibrium constant involving partial pressures,	44
K_T	thermal diffusion ratio,	1
L	length of thermal diffusion tube,	52
L_{ik}	Onsager coefficient,	38
M_i	molar mass of component i,	32
M	$= M_1 x_1 + M_2 x_2$, molar mass of mixture,	40
N	mole fraction, only in chapters I and II,	1
N_1, N_2	mole fraction at T_1 and T_2 respectively,	1
N_o, N_z	mole fraction at $z = 0$ and $z = Z$,	8
N_p	mole fraction of product in a column,	2
N_t	mole fraction at time t,	20
N_A	Avogadro's constant,	45
P	production rate of thermal diffusion column,	2
Pr	Prandtl number,	13
Q	equilibrium separation factor,	1
Q_i^*	heat of transfer, according to Kotousov,	41
R	gas constant per mole,	1
Re	Reynolds number,	13
T	temperature,	1
T_1, T_2	temperature of cold and hot side respectively,	1
$\overline{T}$	mean temperature,	2
ΔT	temperature difference $T_2 - T_1$,	4
T^*	reduced temperature kT/ε,	34
V	molar volume,	41
V_i	molar volume of component i,	42
$\overrightarrow{X_k}$, $\overrightarrow{X_u}$	thermodynamic forces or affinities,	38

Z	length of thermal diffusion column,	5
α	thermal diffusion factor,	1
α_o	thermal diffusion factor at low densities,	40
α_d	degree of dissociation,	45
ε	half "Trennschärfe",	5
ε	potential energy of the minimum in the function of the Lennard - Jones potential model,	33
$\varepsilon(\vec{r}, t)$	local energy density,	35
η	coefficient of viscosity,	4
λ	coefficient of thermal conductivity,	4
μ_i	chemical potential of component i per unit mass,	38
$\tilde{\mu}_i$	molar chemical potential of component i,	40
ρ	density of gas,	4
ρ_i	density of component i,	38
σ	distance of closest approach of two molecules,	33
τ	amount of isotope flowing through a cross section of the column per unit of time,	2
$\phi(r)$	potential energy of interaction between two molecules at distance r,	33
χ	angle by which molecules are deflected,	32
Ψ	normalized production rate P/c_1,	9
$\vec{\psi}_j$	flux vector,	32
$\Omega^{(l,r)}_{i,j}$	collision integral,	13

REFERENCES

1) Chapman, S. and Dootson, F.W., Phil. Mag. 33 (1917) 248.
2) Grew, K.E. and Ibbs, T.L., Thermal diffusion in gases, Cambridge University Press, London and New York (1952).
3) Grove, G.R., Thermal diffusion: a bibliography, Mound Laboratory, Miamisburg, Ohio U.S.A. (1959).
4) Mason, E.A., Munn, R.J. and Smith, F.J., Thermal diffusion in gases, Institute for Molecular Physics, Univ. of Maryland (1965).
5) Clusius, K. and Dickel, G., Naturwiss. 26 (1938) 546.
6) Grotendorst, H.W., Heymann, D., Kistemaker, J., Los, J., Velds, C.A. and De Vries, A.E., J. nuclear Energy A/B 19 (1965) 235.
7) Drickamer, H.G., Mellow, E.W. and Tung, L.H., J. chem. Phys. 18 (1950) 945.
8) Hirota, K. and Kobayashi, Y., J. chem. Phys. 21 (1953) 246; J. chem. Soc. Japan 74 (1953) 604.
9) a. Pierce, N.C., Duffield, R.B. and Drickamer, H.G., J. chem. Phys. 18 (1950) 950.
   a. Giller, E.B., Duffield, R.B. and Drickamer, H.G., J. chem. Phys. 18 (1950) 1027, 1683.
   b. Robb, W.L. and Drickamer, H.G., J. chem. Phys. 18 (1950) 1380; 19 (1951) 818.
   a. Tung, L.H. and Drickamer, H.G., J. chem. Phys. 18 (1950) 1031.
   b. Caskey, F.E. and Drickamer, H.G., J. chem. Phys. 21 (1953) 153.
10) Becker, E.W. and Schulzeff, A., Naturwiss. 35 (1948) 218.
11) Becker, E.W., Z. Naturforsch. 5a (1950) 457; J. chem. Phys. 19 (1951) 131.
12) a. Drickamer, H.G. and Hofto, J.R., J. chem. Phys. 17 (1949) 1165.
   b. Walther, J.E. and Drickamer, H.G., J. phys. Chem. 62 (1958) 421.
13) Makita, T., Rev. phys. Chem. Japan 29 (1960) 47, 55.
   Makita, T. and Takagi, T., ibid. 32 (1963) 1.
14) Van Itterbeek, A., Van Ee, H. and Beenakker, J.J.M., Bull. Inst. Int. Froid Annexe 1 (1958) 275.
   Van Ee, H., Thesis, University of Leiden (1966).
15) Haase, R., Z. Physik 127 (1949) 1; Z. Elektrochem. 54 (1950) 450; Z. phys. Chem. 196 (1950) 219.
16) Enskog, D., Kungl. Svenska Vetenskaps Akad. Handl. 63 no. 4 (1921).
17) Chapman, S. and Cowling, T.G., The mathematical theory of non-uniform gases, Cambridge University Press, London, New York (1952).
18) Hirschfelder, J.O., Curtiss, C.F. and Bird, R.B., Molecular theory of gases and liquids, John Wiley & Sons, Inc., New York (1954).
19) Heymann, D., Thesis, University of Amsterdam (1958).
20) Slieker, C.J.G., Thesis, Technische Hogeschool, Delft (1964).
21) Brown, H., Phys. Rev. 58 (1940) 661.
22) Jones, R.C. and Furry, W.H., Rev. mod. Phys. 18 (1946) 151.

23) Fleischmann, R. and Jensen, H., Erg. exact. Naturw. 20 (1942) 121.
24) Cohen, K., The theory of isotope separation, N.N.E.S., Ser. III, Vol. 1 B. Mc Graw - Hill Book Cy., Inc., New York (1951).
25) Slieker, C.J.G., Z. Naturf. 20 a (1965) 521.
26) Gröber, H., Erk, S. and Grigull, U., Die Grundgesetze der Wärmeübertragung, Springer Verlag, Berlin, Göttingen (1955).
27) Beckmann, W., Forsch. Ing. - Wes. 2 (1931) 165.
28) Sellschopp, W., Forsch. Ing. - Wes. 5 (1934) 162.
29) Kraussold, H., Forsch. Ing. - Wes. 5 (1934) 186.
30) Onsager, L. and Watson, W.W., Phys. Rev. 56 (1939) 474.
31) Donaldson, J. and Watson, W.W., Phys. Rev. 82 (1951) 909.
32) Saxena, S.C. and Mason, E.A., Mol. Phys. 2 (1959) 264, 379.
33) Dickel, G., Z. Naturf. 16 a (1961) 755.
34) Dickel, G. and Bürkholz, A., Z. Naturf. 16 a (1961) 760.
35) Cremer, E., Z. anorg. Chem. 258 (1949) 123.
36) Kihara, T., Imperfect gases, Asakusa Bookstore, Tokyo (1949); ref. no. 18, p. 608.
37) Lugg, J.W.H., Phil. Mag. 8 (1929) 1019.
38) Ibbs, T.L., Grew, K.E. and Hirst, A.A., Proc. phys. Soc. 41 (1929) 456.
39) Grew, K.E., Nature 156 (1945) 267.
40) Bogoliubov, N.N., J. Phys. USSR 10 (1946) 265.
Studies in Statistical Mechanics I, North-Holland Publ. Cy., Amsterdam (1962) 5.
41) Choh, S.T. and Uhlenbeck, G.E., Navy theor. phys. contract no. Nonr. 1224 (15) 1958; Dissertation, Univ. of Michigan (1958).
42) Green, M.S., J. chem. Phys. 25 (1956) 836; Physica 24 (1958) 393.
43) Cohen, E.G.D., Physica 28 (1962) 1025, 1045, 1060; J. math. Phys. 4 (1963) 183.
44) García - Colin, L.S., Green, M.S. and Chaos, F., Physica 32 (1966) 450.
45) Mori, H., Studies in Statistical Mechanics I, North-Holland Publ. Cy., Amsterdam (1962) 271.
46) Kirkwood, J.G. and Fitts, D.D., J. chem. Phys. 33 (1960) 1317.
47) Green, H.S., J. math. Phys. 2 (1961) 344.
48) Mc Lennan, J.A., Advances in Chemical Physics V, Interscience Publ., New York (1963) 261.
49) Kubo, R., J. phys. Soc. Japan 12 (1957) 570.
50) Ernst, M.H.J.J., Dorfman, J.R. and Cohen, E.G.D., Physica 31 (1965) 493; Ernst, M.H.J.J., Physica 32 (1966) 209.
51) Ono, S., Proceed. Intern. Symp. on Statist. Mech. and Thermodynamics, Aachen 1964, ed. J. Meixner, North-Holland Publ. Cy., Amsterdan (1965) 126.
52) Cohen, E.G.D., Proceed. Intern. Symp. on Statist. Mech. and Thermodynamics, Aachen 1964, ed. J. Meixner, North-Holland Publ. Cy., Amsterdam (1965) 140.
53) Prigogine, I., Résibois, P. and Severne, G., Phys. Letters 9 (1964) 317; Résibois, P., J. chem. Phys. 41 (1964) 2979.

54) Cohen, E.G.D., to be published.
55) Kotousov, L.S., L.P.I. Fiz. - mekh. fak., n. - tekh. informats. byull. 8 (1959) 15; Sov. Phys. - Techn. Phys. 7 (1962) 58; 9 (1965) 1694.
56) De Groot, S.R., Thermodynamics of irreversible processes, North-Holland Publ. Cy., Amsterdam (1961).
57) Wall, F.T. and Stent, G.S., J. chem. Phys. 17 (1949) 1112.
58) Leckenby, R.E. and Robbins, E.J., Proc. roy. Soc. A 291 (1966) 389.
59) Stogryn, D.E. and Hirschfelder, J.O., J. chem. Phys. 31 (1959) 1545.
60) Kim, S.K. and Ross, J., J. chem. Phys. 42 (1965) 263;
Kim, S.K., Flynn, G.P. and Ross, J., J. chem. Phys. 43 (1965) 4166.
61) Van der Valk, F., Physica 29 (1963) 417.
62) Baranovski, B. and De Vries, A.E., Physica, to be published.
63) Slieker, C.J.G. and De Vries, A.E., J. du Chim. phys. 60 (1963) 172.
64) Ghozlan, A.I., Thesis, University of Leiden (1963).
65) Elliott, G.A. and Masson, I., Proc. roy. Soc. (London) A 108 (1925) 378.
66) Franck, E.U., Chem. Ing. Technik 25 (1953) 238.
67) Michels, A., Sengers, J.V. and Van der Gulik, P.S., Physica 28 (1962) 1216.
68) Beattie, J.A. and Bridgeman, O.C., J. Amer. chem. Soc. 49 (1927) 1665; Proc. Amer. Acad. Arts Sci 63 (1928) 229.